

# Multi-layer State Evolution Under Random Convolutional Design

Max Daniels<sup>\*1</sup>, Cédric Gerbelot<sup>\*2</sup>, Florent Krzakala<sup>2</sup>, and Lenka Zdeborová<sup>3</sup>

<sup>1</sup>College of Computer Science and Department of Mathematics, Northeastern University, 02120 Boston, USA

<sup>2</sup>Ecole Polytechnique Fédérale de Lausanne (EPFL), Information, Learning and Physics (IdePHics) Laboratory, CH-1015 Lausanne, Switzerland

<sup>3</sup>Ecole Polytechnique Fédérale de Lausanne (EPFL), Statistical Physics of Optimization (SPOC) Laboratory, CH-1015 Lausanne, Switzerland

## Abstract

Signal recovery under generative neural network priors has emerged as a promising direction in statistical inference and computational imaging. Theoretical analysis of reconstruction algorithms under generative priors is, however, challenging. For generative priors with fully connected layers and Gaussian i.i.d. weights, this was achieved by the multi-layer approximate message (ML-AMP) algorithm via a rigorous state evolution. However, practical generative priors are typically convolutional, allowing for computational benefits and inductive biases, and so the Gaussian i.i.d. weight assumption is very limiting. In this paper, we overcome this limitation and establish the state evolution of ML-AMP for random convolutional layers. We prove in particular that random convolutional layers belong to the same universality class as Gaussian matrices. Our proof technique is of an independent interest as it establishes a mapping between convolutional matrices and spatially coupled sensing matrices used in coding theory.

## 1 Introduction

In a typical signal recovery problem, one seeks to recover a data signal  $x_0$  given access to measurements  $y_0 = G_\theta(x_0)$ , where the parameters  $\theta$  of the signal model are known. In many problems, it is natural to view the measurement generation process as a composition of simple forward operators, or ‘layers.’ In this work, we are concerned with multi-layer signal models of the form

$$G_\theta(h) = \varphi^{(1)}(W^{(1)}\varphi^{(2)}(W^{(2)} \dots \varphi^{(L)}(W^{(L)}h))). \quad (1)$$

where  $W^{(l)} \in \mathbb{R}^{n_{l-1} \times n_l}$  are linear sensing matrices and where  $\varphi^{(l)}(z)$  are separable, possibly non-linear channel functions. In the  $L = 1$  case, this signal model naturally generalizes problems such as phase retrieval  $\varphi(z) = |z|$  or compressive sensing  $\varphi(z) = z$ , and for multi-layer models  $L > 1$ ,  $G_\theta(h)$  may be viewed as a deep neural network.

Recently, convolutional Generative Neural Networks (GNNs) have shown promise as generalizations of sparsity priors for a variety of signal processing applications [Bora et al., 2017]. Motivated by this success, we take interest in a variant of the recovery problem (1) in which some of the sensing matrices  $W^{(l)}$  may be *multi-channel convolutional* (MCC) matrices, having a certain block-sparse circulant structure which captures the convolutional layers used by many modern generative neural network architectures [Karras et al., 2018, 2019].

<sup>\*</sup>The first two authors contributed equally to this work.

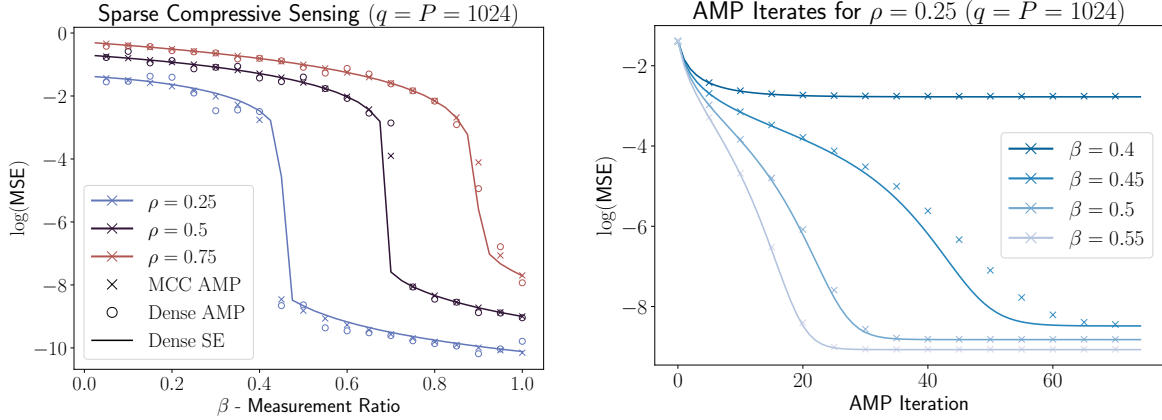


Figure 1: Agreement between the performance of the AMP algorithm run with random multichannel convolutional matrices and its state evolution as proven in this paper. **(left)** Compressive sensing  $y_0 = Wx_0 + \zeta$  for noise  $\zeta_i \sim \mathcal{N}(0, 10^{-4})$  and signal prior  $x_0 \sim \rho\mathcal{N}(0, 1) + (1 - \rho)\delta(x)$ , where  $W \in \mathbb{R}^{Dq \times Pq}$  has varying aspect ratio  $\beta = D/P$ . Crosses correspond to AMP evaluations for  $W \sim \text{MCC}(D, P, q, k)$  according to Definition 3.2, averaged over 10 independent trials. Dots correspond to AMP evaluations for  $W \in \mathbb{R}^{D \times P}$  with i.i.d. Gaussian entries  $W_{ij} \sim \mathcal{N}(0, 1/Pq)$ . Lines show the state evolution predictions when  $W_{ij} \sim \mathcal{N}(0, 1/Pq)$ . The system size is  $P = 1024$ ,  $q = 1024$ ,  $k = 3$ , where  $\beta$  and  $D = \beta P$  vary. While our theorem treats the limit  $P, D \rightarrow \infty$ ,  $q, k = O(1)$ , we observe strong empirical agreement even when  $q \sim P$ . In Appendix C.1 we give the same figure for  $q = 10 \ll P$ . **(right)** AMP iterates at  $\rho = 0.25$  and  $\beta$  near the recovery transition. Rather than showing these models have equivalent fixed points, we show a stronger result: the state evolution equations are equivalent *at each iteration*.

In this work, we develop an asymptotic analysis of the performance of an *Approximate Message Passing* (AMP) algorithm [Donoho et al., 2009] for recovery from multichannel convolutional signal models. This family of algorithms originates in statistical physics [Mézard and Montanari, 2009; Zdeborová and Krzakala, 2016] and allows to compute the marginals of an elaborate posterior distribution defined by an inference problem involving dense random matrices. A number of AMP iterations have been proposed for various inference problems, such as compressed sensing [Donoho et al., 2009], low-rank matrix recovery [Rangan and Fletcher, 2012] or generalized linear modeling [Rangan, 2011]. More recently, composite AMP iterations (ML-AMP) have been proposed to study multilayer inference problems [Manoel et al., 2017; Aubin et al., 2019]. Here we consider the ML-AMP proposed in [Manoel et al., 2017] to compute marginals of a multilayer generalized linear model, however the usual dense Gaussian matrices will be replaced by random convolutional ones. A major benefit of AMP lies in the fact that the asymptotic distribution of their iterates can be exactly determined by a low-dimensional recursion: the state evolution equations. This enables to obtain precise theoretical results for the reconstruction performance of the proposed algorithm. Another benefit of such iterations is their low computational complexity, as they only involve matrix-multiplication and, in the separable case, pointwise non-linearities.

Previous works on AMP suggest that the state evolution is not readily applicable to our setting because its derivation requires strong independence assumptions on the coordinates of the  $\{W^{(l)}\}$  which are violated by structured multi-channel convolution matrices. Despite this, we use AMP for our setting and rigorously prove its state evolution. Our main contributions are:

1. We rigorously prove state evolution equations for models of the form (1), where weights are allowed to be either i.i.d. Gaussian or random structured MCC matrices, as in Definition 3.2.
2. For separable channel functions  $\varphi^{(l)}$  and separable signal priors, we show that the original ML-AMP of [Manoel et al., 2017] used with dense Gaussian matrices or random convolutional ones admits the same state evolution equations, up to a rescaling. Multi-layer MCC signal models can

therefore simulate dense signal models while making use of fast structured matrix operations for convolutions.

3. The core of our proof shows how an AMP iteration involving random convolutional matrices may be reduced to another one with dense Gaussian matrices. We first show that random convolutional matrices are equivalent, through permutation matrices, to dense Gaussian ones with a (sparse) block-circulant structure. We then show how the block-circulant structure can be embedded in a new, matrix-valued, multilayer AMP with dense Gaussian matrices, the state evolution equations of which are proven using the results of [Gerbelot and Berthier, 2021], with techniques involving spatially coupled matrices [Krzakala et al., 2012; Javanmard and Montanari, 2013].
4. We validate our theory numerically and observe close agreement between convolutional AMP iterations and its state evolution predictions, as shown in Figure 1 and in Section 5. Our code can be used as a general purpose library to build compositional models and evaluate AMP and its state evolution. We make this code available at <https://github.com/mdnls/conv-ml-amp>.

## 2 Related Work

AMP-type algorithms arose independently in the contexts of signal recovery and spin-glass theory. In the former case, [Donoho et al., 2009] derives AMP for Gaussian compressive sensing. This approach was later generalized by [Rangan, 2011] to recovery problems with componentwise *channel functions* that may be stochastic and/or nonlinear, and generalized further by [Manoel et al., 2017] to multi-layer or compositional models. Due to the versatility of this approach, a wide variety of general purpose frameworks for designing AMP variants have since been popularized [Fletcher et al., 2018; Baker et al., 2020; Gerbelot and Berthier, 2021]. Proof techniques to show the concentration of AMP iterates to the state evolution prediction developed alongside new variants of the algorithm. In the context of spin-glass theory, Bolthausen’s seminal work [Bolthausen, 2009] introduces a Gaussian conditioning technique used widely to prove AMP concentration. Following this approach, [Bayati and Montanari, 2011; Javanmard and Montanari, 2013; Berthier et al., 2020] treat signal models with dense couplings and generalized channel functions. More recently, a proof framework adaptable to composite inference problems was proposed in [Gerbelot and Berthier, 2021], which we use in our proof.

There has also been significant interest in relaxing the strong independence assumptions required by AMP algorithms on sensing matrix coordinates. In one direction, *Vector AMP* (VAMP) algorithms target signal models whose sensing matrices are drawn from *right orthogonally invariant* distributions. The development of VAMP algorithms followed a similar trajectory to that of vanilla AMP [Schniter et al., 2016; Fletcher et al., 2018; Rangan et al., 2019; Baker et al., 2020]. The MCC ensemble considered in this work is not right orthogonally invariant, but we observe strong empirical evidence that an analogous version of Theorem 4.2 holds for VAMP as well, as described in Appendix C.2. In a second direction, there has been much interest in *spatial coupling* sensing matrices, which were used to achieve the information-theoretically optimal performance in sparse compressive sensing [Donoho et al., 2013; Barbier et al., 2015; Krzakala et al., 2012], with complementary state evolution guarantees [Javanmard and Montanari, 2013]. The concept of spatial coupling and proofs of its performance originated in the literature of error correcting codes [Kudekar et al., 2011, 2013], where it developed from the so-called convolutional codes [Felstrom and Zigangirov, 1999]. The connection between spatial coupling and convolution layers of neural networks, that we establish in this paper, is as far as we know novel.

Another direction of related work is the design of generative neural network architectures, and correspondingly, the design of signal recovery procedures that can make use of new generative prior models. There is a wide variety of architectures for feedforward convolutional generative priors, which are often hand-crafted to be stably trained on real world datasets. For instance, the DC-GAN architecture, studied by Bora et al. [2017] in compressive sensing and superresolution tasks, achieves stable training through the use of multi-channel *strided* convolutional layers and batch normalization [Radford et al., 2015]. Following this, the PG-GAN architecture [Karras et al., 2018] uses multichannel convolutional

layers, upsampling layers, and a parameter free alternative to batch normalization. Recently, Style-GAN has emerged as a popular architecture for generating large, high-resolution images [Karras et al., 2019]. The StyleGAN generator uses residual and skip connections to encourage a hierarchical image generation process, contributing to stable training even when generating high resolution images. Style-GAN and PG-GAN, and further domain-specific modifications, have been studied as priors for a variety of signal recovery problems [Daras et al., 2021; Gu et al., 2020]. For simplicity and theoretical tractability, we do not consider fine-grained practical modifications like batch normalization or strided convolution, focusing instead on the essential elements of simple convolutional networks. Lastly, while our focus is on feedforward convolutional priors such as GAN/VAE networks, there is growing interest in alternative approaches to signal recovery under neural network priors, such as normalizing flows [Kingma and Dhariwal, 2018; Asim et al., 2020] and score-based generative models [Song and Ermon, 2020; Jalal et al., 2021]. These approaches fall outside the scope of our work and may be interesting directions for future investigation.

### 3 Definition of the problem

#### 3.1 Multi-channel Convolutional Matrices

We focus our attention on *multichannel convolution matrices* that have *localized convolutional filters*. In this section, we introduce our notation and define the random matrix ensembles which are relevant to our result. We consider block structured signal vectors  $x \in \mathbb{R}^{Pq}$  of the form  $x = [x^{(i)}]_{i=1}^P$ , and we refer to the blocks  $x^{(i)} \in \mathbb{R}^q$  as ‘channels.’ For any vector of dimension  $d$ , we denote by  $\mathcal{P}_d \in \mathbb{R}^{d \times d}$  the cyclic coordinate permutation matrix of order  $d$ , whose coordinates are  $\langle e_i, \mathcal{P}_d e_j \rangle = \mathbf{1}[i = j + 1]$ . For a block-structured vector  $x \in \mathbb{R}^{Pq}$ , we denote by  $\mathcal{P}_{P,q} \in \mathbb{R}^{Pq \times Pq}$  the block cyclic permutation matrix satisfying  $(\mathcal{P}_{P,q} x)^{(i)} = x^{(i+1)}$  for  $1 \leq i < P$ , and  $(\mathcal{P}_{P,q} x)^{(P)} = x^{(1)}$ . Similarly, we denote by  $\mathcal{S}_{i,j} \in \mathbb{R}^{Pq \times Pq}$  the swap permutation matrix which exchanges blocks  $i, j$ :  $[\mathcal{S}_{i,j} x]^{(i)} = x^{(j)}$ ,  $[\mathcal{S}_{i,j} x]^{(j)} = x^{(i)}$ , and  $[\mathcal{S}_{i,j} x]^{(k)} = x^{(k)}$  for  $k \neq i, j$ . Last, given a vector  $\omega \in \mathbb{R}^k$  for  $k \leq q$ , denote by  $\text{Zero-Pad}_{q,k}(\omega)$  the vector whose first  $k$  coordinates are  $\omega$ , and whose other coordinates are zero.

$$\text{Zero-Pad}_{q,k}(\omega) = [\omega_1 \ \omega_2 \ \dots \ \omega_k \ 0 \ \dots \ 0] \in \mathbb{R}^q.$$

We define the following ensemble for random multi-channel convolution matrices.

**Definition 3.1** (Gaussian i.i.d. Convolution). Let  $q \geq k$  be integers. The convolutional ensemble  $\mathcal{C}(q, k)$  contains random circulant matrices  $C \in \mathbb{R}^{q \times q}$  whose first row is given by  $C_1 = \text{Zero-Pad}_{q,k}[\omega]$  where  $\omega \in \mathbb{R}^k$  has i.i.d. Gaussian coordinates  $\omega_i \sim \mathcal{N}(0, 1/k)$ . The remaining rows  $C_i$  are determined by circulant structure, ie.  $C_i = \mathcal{P}_q^{i-1} \text{Zero-Pad}_{q,k}[\omega]$ .

Random multi-channel convolutions are block-dense matrices with independent  $\mathcal{C}(q, k)$  blocks.

**Definition 3.2** (Multi-channel Gaussian i.i.d. Convolution). Let  $D, P \geq 1$  and  $q \geq k \geq 1$  be integers. The random multi-channel convolution ensemble  $\mathcal{M}(D, P, k, q)$  contains random block matrices  $M \in \mathbb{R}^{Dq \times Pq}$  of the form

$$M = \frac{1}{\sqrt{P}} \begin{bmatrix} C_{1,1} & C_{1,2} & \dots & C_{1,P} \\ C_{2,1} & \ddots & & \vdots \\ \vdots & & & \\ C_{D,1} & \dots & & C_{D,P} \end{bmatrix}$$

where each  $C_{i,j} \sim \mathcal{C}(q, k)$  is sampled independently.

Fig. 2 gives a graphical explanation of the link between these matrices and the convolutional layers. The parameter  $P$  ( $D$ ) is the number of input (output) channels,  $q$  is the dimension of the input and  $k$  the filter size.

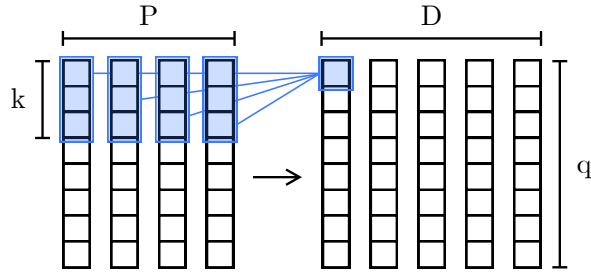


Figure 2: MCC matrices operate on  $Pq$  dimensional input data, composed of  $q$ -dimensional signals for each of  $P$  separate channels. The  $i$ -th output channel is a linear combination of convolutional features extracted from input channels, where  $k$  is the convolutional filter size:  $y^{(i)} = \sum_{j=1\dots P} C_{ij}x^{(j)}$ . Blue boxes show linear dependencies between signal coordinates.

Layer	$D$	$P$	$q$	$k$
1 $\rightarrow$ 2	1024	512	$4^2$	1
2 $\rightarrow$ 3	512	256	$8^2$	5
3 $\rightarrow$ 4	256	128	$16^2$	5
4 $\rightarrow$ 5	128	3	$64^2$	5

Figure 3: System sizes for convolutional layers in a DC-GAN architecture used to generate LSUN images [Radford et al., 2015, Figure 1]. These are *not* directly comparable to MCC matrices, as DCGAN uses *fractionally strided convolutions*, which can be thought of as a composition of an MCC matrix with superresolution. However, they give a reasonable picture of the sizes of typical layers in convolutional neural networks.

### 3.2 Thermodynamic-like Limit and Finite-size Regimes

We prove our main result in a thermodynamic-like limit  $D, P \rightarrow \infty$  while  $\beta = D/P$  is fixed and  $q, k = O(1)$ . From a practical perspective, convolutional layers in deep neural networks often use large channel dimensions ( $D, P \gg 1$ ), large signal dimensions ( $q \gg 1$ ), and a small filter size ( $k = O(1)$ ). As an example, we show in Figure 3 the sizes of convolutional layers used by the DC-GAN architecture to generate LSUN images [Radford et al., 2015, Figure 1].

Interestingly, our theoretical predictions do not depend explicitly on the *relative* sizes of  $q$  and  $(D, P)$ . We observe empirically that these predictions become accurate at finite sizes of  $(D, P)$  which may seem small relative to  $q$ , and which are realistic from a practical neural network perspective. For example, in Figure 1, we observe strong empirical agreement with predictions for  $q = P = 1024$  as  $\beta$  and  $D = \beta P$  vary.

### 3.3 Multi-layer AMP

In this section, we define a class of probabilistic graphical models (PGMs) that captures the inference problems of interest, and we state the Multi-layer Approximate Message Passing (ML-AMP) [Manoel et al., 2017] iterations, which can be used for inference on these PGMs. We consider the following signal model.

**Definition 3.3** (Multi-layer Signal Model). Let  $\{W^{(l)}\}_{1 \leq l \leq L}$  be matrices of dimension  $W^{(l)} \in \mathbb{R}^{n_{l-1} \times n_l}$ . Let  $\{\varphi_\zeta^{(l)}(z)\}_{1 \leq l \leq L}$  be scalar channel functions  $\varphi_\zeta^{(l)} : \mathbb{R} \rightarrow \mathbb{R}$  for which  $z$  is the estimation quantity and  $\zeta$  represents channel noise. We write  $\varphi_\zeta^{(l)}(z)$  for vectors  $z \in \mathbb{R}^{n_{l-1}}$  to indicate the coordinatewise application of  $\varphi^{(l)}$ . The multi-layer GLM signal model is given by

$$y = \varphi_\zeta^{(1)}(W^{(1)}\varphi_\zeta^{(2)}(W^{(2)}(\dots\varphi_\zeta^{(L)}W^{(L)}x))).$$

We assume  $x \in \mathbb{R}^{nL}$  follows a known separable prior,  $x_i \sim P_X(x)$  i.i.d., and that  $\zeta \sim \mathcal{N}(0, 1)$ .

The full estimation quantities of the model are the coordinates of the vectors  $\{h^{(l)}\}_{1 \leq l \leq L}$ ,  $\{z^{(l)}\}_{1 \leq l \leq L}$ , which are related by

$$\begin{aligned} y_\mu &= \varphi_\zeta^{(1)}(z^{(1)}) & z_\mu^{(1)} &= \sum_i W_{\mu i}^{(1)} h_i^{(1)}, \\ h_i^{(1)} &= \varphi_\zeta^{(2)}(z^{(2)}) & z_\mu^{(2)} &= \sum_i W_{\mu i}^{(2)} h_i^{(2)}, \\ &\vdots & & \\ h_i^{(L-1)} &= \varphi_\zeta^{(L)}(z^{(L)}) & z_\mu^{(L)} &= \sum_i W_{\mu i}^{(L)} x_i \end{aligned} \quad (2)$$

and the corresponding conditional probabilities, which define the factor nodes of the underlying PGM, are given by

$$P^{(l)}(h | z) = \int d\zeta e^{-\frac{1}{2}\zeta^2} \delta(h - \varphi_\zeta(z)).$$

To compute the posterior marginals, ML-AMP iteratively updates the parameters of independent 1D Gaussian approximations to each marginal. Each coordinate  $h_i^{(l)}(t)$  has corresponding parameters  $\{A_i^{(l)}(t), B_i^{(l)}(t)\}$  and each  $z_\mu^{(l)}(t)$  has corresponding  $\{V_\mu^{(l)}(t), \omega_\mu^{(l)}(t)\}$ , where  $t \geq 1$  indexes the ML-AMP iterations. The recursive relationship between these parameters is defined in terms of scalar *denoising functions*,  $\hat{h}^{(l)}$  and  $g^{(l)}$ , which compute posterior averages of the estimation quantities given their prior parameters.

In general, these denoising functions can be chosen (up to regularity assumptions) to adjust ML-AMP's performance in applied settings, such as in [Metzler et al., 2015], and in these cases the denoisers may be nonseparable vector valued functions. However, in the separable, Bayes-optimal regime where  $P_x(x)$  and  $P^{(l)}(h | z)$  are known, the optimal denoisers are given by,

$$\begin{aligned} \hat{h}_i^{(l)}(t+1) &:= \partial_B \log \mathcal{Z}^{(l+1)}(A_i^{(l)}, B_i^{(l)}, V_i^{(l+1)}, \omega_i^{(l+1)}) \\ \sigma_i^{(l)}(t+1) &:= \partial_B \hat{h}_i^{(l)}(t+1) \\ g_\mu^{(l)}(t) &:= \partial_\omega \log \mathcal{Z}^{(l)}(A_\mu^{(l-1)}, B_\mu^{(l-1)}, V_\mu^{(l)}, \omega_\mu^{(l)}) \\ \eta_\mu^{(l)}(t) &:= \partial_\omega g_\mu^{(l)}(t) \\ \mathcal{Z}^{(l)}(A, B, V, \omega) &:= \frac{1}{\sqrt{2\pi V}} \int P^{(l)}(h | z) \exp\left(Bh - \frac{1}{2}Ah^2 - \frac{(z - \omega)^2}{2V}\right) dh dz \end{aligned} \quad (3)$$

where  $2 \leq L \leq L-1$ ,  $t \geq 2$  and the prior parameters on the right hand side are taken at iteration  $t \geq 2$ . The corresponding ML-AMP iterations are given by,

$$\begin{aligned} V_\mu^{(l)}(t) &= \sum_i [W_{\mu i}^{(l)}]^2 \sigma_i^{(l)}(t) & \omega_\mu^{(l)}(t) &= \sum_i W_{\mu i}^{(l)} \hat{h}_i^{(l)}(t) - V_\mu^{(l)}(t) g_\mu^{(l)}(t-1) \\ A_i^{(l)}(t) &= -\sum_\mu [W_{\mu i}^{(l)}]^2 \eta_\mu^{(l)}(t) & B_i^{(l)}(t) &= \sum_\mu W_{\mu i}^{(l)} g_\mu^{(l)}(t) + A_i^{(l)}(t) \hat{h}_i^{(l)}(t). \end{aligned} \quad (4)$$

For the boundary cases  $t = 1$ ,  $l = 1$ , and  $l = L$ , the iterations (3), (4) are modified as follows.

1. At  $t = 1$ , we initialize  $B_i^{(l)} \sim P_{B_0}^{(l)}$  and  $\omega_\mu^{(l)} \sim P_{\omega_0}^{(l)}$ , where  $P_{B_0}^{(l)}, P_{\omega_0}^{(l)}$  are the distributions of the signal model parameters (2) when  $x_i \sim P_X$ . We take  $(A_i^{(l)})^{-1} = \text{Var}(B_i^{(l)})$  and  $V_\mu^{(l)} = \text{Var}(\omega_\mu^{(l)})$ .
2. At  $l = 1$ , the denoiser  $g_\mu^{(1)}(t) = \partial_\omega \log \mathcal{Z}^{(1)}(y, V_\mu^{(1)}, \omega_\mu^{(1)})$ , where

$$\mathcal{Z}^{(1)}(y, V_\mu^{(1)}, \omega_\mu^{(1)}) = \frac{1}{\sqrt{2\pi V}} \int P^{(1)}(y | z) \exp\left(-\frac{(z - \omega_\mu^{(1)})^2}{2V_\mu^{(1)}}\right) dz.$$

3. At  $l = L$ , the denoiser  $\hat{h}^{(L)}(t) = \partial_B \log \mathcal{Z}^{(L)}(A_i^{(L)}, B_i^{(L)})$ , where

$$\mathcal{Z}^{(L)}(A_i^{(L)}, B_i^{(L)}) = \int P_X(h) \exp\left(B_\mu^{(L)} h - \frac{1}{2} A_\mu^{(L)} h^2\right) dh.$$

### 3.3.1 Computational Savings of MCC Matrices

As ML-AMP requires only matrix-vector products, its computational burden can be significantly reduced when using structured and/or sparse sensing matrices. In our setting, multi-channel convolutions  $M \sim \text{MCC}(D, P, q, k)$  have  $DPk$  independent, nonzero coordinates, compared to  $DPq^2$  nonzero coordinates of a Gaussian i.i.d. matrix. Typically,  $k$  represents the size of a localized filter applied to a larger image, with  $k \ll q$  [Gonzalez and Woods, 2008, Section 3.4], leading to significant space savings by a factor  $k/q^2$ . This same is true in convolutional neural networks, where the use of localized convolutional filters represents an inductive bias towards localized features that is considered a key aspect of their practical success [Krizhevsky et al., 2012; Zeiler and Fergus, 2014].

In addition to space savings, specialized matrix-vector product implementations can reduce the time complexity of ML-AMP with MCC sensing matrices. Simple routines for sparse matrix-vector products run in time proportional to the number of nonzero entries, resulting in the same  $k/q^2$  constant factor speed up for MCC matrix-vector products. Alternatively, if  $k \gg \log q$ , then a simple algorithm using a fast Fourier transform for convolution-vector products yields time complexity  $O(DPq \log q)$ . Such an algorithm is sketched Appendix B.

## 4 Main result

We now state our main technical result, starting with the set of required assumptions.

(A1) for any  $1 \leq l \leq L$ , the function  $\varphi^l$  is continuous and there exists a polynomial  $b^{(l)}$  of finite order such that, for any  $x \in \mathbb{R}$ ,  $|\varphi^{(l)}(x)| \leq |b^{(l)}(x)|$

(A2) for any  $1 \leq l \leq L$ , the matrix  $\mathbf{W}^{(l)}$  is sampled from the ensemble  $\mathcal{M}(D^l, P^l, k^l, q^l)$  where  $P^l q^l = D^{l-1} q^{l-1}$

(A3) the iteration 4 is initialized with a random vector independent of the mixing matrices verifying  $\frac{1}{N} \|\mathbf{h}_0\|_2^2 < +\infty$  almost surely

(A4) for any  $1 \leq l \leq L$ ,  $D_l, P_l \rightarrow \infty$  with constant ratio  $\beta_l = D_l/P_l$ , with finite  $q_l$ .

Under these assumptions, we may define the following *state evolution* recursion

**Definition 4.1** (State Evolution). Consider the following recursion,

$$\hat{m}^{(l)}(t) = -\beta^{(l)} \mathbb{E}^{(l)}[\partial_\omega g(\hat{m}^{(l-1)}, \hat{m}b, \tau_1 - m^{(l)}, h)] \quad (5)$$

$$m^{(l-1)}(t+1) = \mathbb{E}^{(l)}[h \hat{h}^{(l-1)}(\hat{m}^{(l-1)}, \hat{m}b, \tau_1 - m^{(l)}, h)], \quad (6)$$

where  $\tau^{(l)}$  is the second moment of  $P_{B_0}^{(l)}$ , where the right hand side parameters are taken at time  $t$ , and the expectations  $\mathbb{E}^{(l)}$  are taken with respect to

$$P^{(l)}(w, z, h, b) = P_{\text{out}}^{(l)}(h | z) \mathcal{N}(z; w, \tau^{(l)} - m^{(l)}) \mathcal{N}(w; 0, m^{(l)}) \mathcal{N}(b; \hat{m}^{(l-1)} h, \hat{m}^{(l-1)}).$$

At  $t = 1$ , the state evolution is initialized at  $\kappa^{(l)} = 0$  and  $(\hat{\kappa}^{(l)})^{-1} = \tau^{(l)}$ . At the boundaries  $l = 1, L$ , the expectations are modified analogously to the ML-AMP iterations as described by Manoel et al. [2017]. We then have the following asymptotic characterization of the iterates from the convolutional ML-AMP algorithm

**Theorem 4.2.** Under the set of assumptions (A1)-(A4), for any sequences of uniformly pseudo-Lipschitz functions  $\psi_1^N, \psi_2^N$  of order  $k$ , for any  $1 \leq l \leq L$  and any  $t \in \mathbb{N}$ , the following holds

$$\frac{1}{D_l q_l} \sum_{i=1}^{D_l q_l} \psi_1(\omega_i^{(l)}(t)) \stackrel{P}{\simeq} \mathbb{E} \left[ \psi_1 \left( Z^l(t) \right) \right] \quad (7)$$

$$\frac{1}{P_l q_l} \sum_{i=1}^{P_l q_l} \psi_2(B_i^{(l)}(t)) \stackrel{P}{\simeq} \mathbb{E} \left[ \psi_2 \left( \hat{Z}^l(t) \right) \right] \quad (8)$$

where  $Z^l(t) \sim \mathcal{N}(0, \kappa^l(t))$ ,  $\hat{Z}^l(t) \sim \mathcal{N}(0, \hat{\kappa}^l(t))$  are independent random variables.

## 4.1 Proof Sketch

The proof of Theorem 4.2, which is given in Appendix A, has two key steps. First, we construct permutation matrices  $U, \tilde{U}$  such that for  $W \sim \text{MCC}(D, P, q, k)$ , the matrix  $\tilde{W} = U W \tilde{U}^T$  is a block matrix whose blocks either have i.i.d. Gaussian elements or are zero valued, and has a block-circulant structure. The effect of the permutation is that entries of  $\tilde{W}$  which are correlated due to circulant structure of  $W$  are relocated to different blocks. Once these permutation matrices are defined, we define a new, matrix-valued AMP iteration involving the dense Gaussian matrices obtained from the permutations, and whose non-linearities account for the block-circulant structures and the permutation matrices. The state evolution of this new iteration is proven using the results of [Gerbelot and Berthier, 2021]. This provides an explicit example of how the aforementioned results can be used to obtain rigorous, non Bayes-optimal SE equations on a composite AMP iteration. The separability assumption is key in showing that the AMP iterates obtained with the convolutional matrices can be *exactly* embedded in a larger one. Note that this is a stronger result than proving SE equations for an algorithm that computes marginals of a random convolutional posterior: we show the SE equations are the same as in the dense case. We finally invoke the Nishimori conditions, see e.g. [Krzakala et al., 2012], to simplify the generic, non Bayes-optimal SE equations to the Bayes-optimal ones.

The idea of embedding a non-separable effect such as a block-circulant structure or different variances in a mixing matrix is the core idea in the proofs of SE equations for spatially coupled systems, notably as done in [Javanmard and Montanari, 2013; Donoho et al., 2013]. We note that in the numerical experiments shown at Figure 1, the parameter  $q$ , considered finite in the proof, is actually comparable to the number of channel, considered to be extensive. Empirically we observe that this does not hinder the validity of the result, something that was also observed in the spatial coupling literature, e.g. [Krzakala et al., 2012], where large number of different blocks in spatially coupled matrices were considered, with convincing numerical agreement.

The existence of permutations matrices verifying the property described above is formalized in the following lemma:

**Lemma 4.3** (Permutation Lemma). Let  $W \sim \mathcal{M}(D, P, k, q)$  be a multi-channel convolution matrix. There exist row and column permutation matrices  $U \in \mathbb{R}^{Dq \times Dq}$ ,  $\tilde{U} \in \mathbb{R}^{Pq \times Pq}$  such that  $\tilde{W} = U W \tilde{U}^T$  is a block-convolutional matrix with dense, Gaussian i.i.d. blocks. That is,

$$\tilde{W} = \frac{1}{\sqrt{k}} \begin{bmatrix} A^{(1)} & A^{(2)} & \dots & A^{(k)} & & \\ & A^{(1)} & A^{(2)} & \dots & A^{(k)} & \\ \vdots & & A^{(2)} & \dots & A^{(k)} & \\ & & & \ddots & & \vdots \\ A^{(2)} & A^{(3)} & \dots & A^{(k)} & & A^{(1)} \end{bmatrix}$$

where each  $A^{(s)} \in \mathbb{R}^{D, P}$ ,  $1 \leq s \leq k$  has i.i.d.  $\mathcal{N}(0, 1/P)$  coordinates.

*Proof.* Consider the elements of the matrix  $M$  which are non-zero and sampled i.i.d. as opposed to exact copies of other variables. They are positioned on the first line of each block of size  $q \times q$ , and thus the



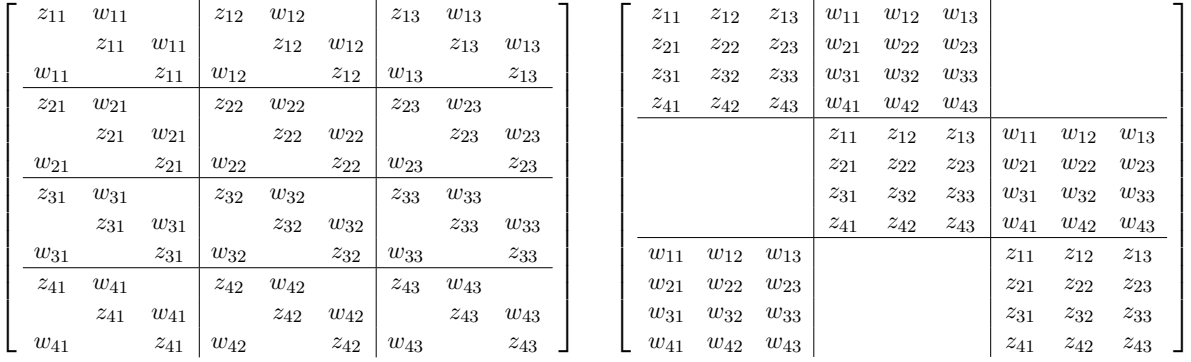


Figure 4: A sketch of the permutation lemma applied to matrix  $W \sim \text{MCC}(4, 3, 3, 2)$ . Left:  $W$  before permutation. Right: after permutation,  $UW\tilde{U}^T$ .

indexing for their lines and columns can be written as  $M_{aq+1,bq+c}$  where  $a, b, c$  are integers such that  $0 \leq a \leq D-1$ ,  $0 \leq b \leq P-1$  and  $1 \leq c \leq k$ . The integers  $a, b$  describe the position of the  $q \times q$  block the variable is in, and  $c$  describes, for each block, the position in the initial random Gaussian vector of size  $k$  that is zero-padded and circulated to generate the block. The goal is to find the mapping that groups these variables into  $k$  dense blocks of extensive size  $D \times P$ . To do so, one can use the following bijection  $\tilde{M}_{\gamma,\alpha P+\beta} = M_{aq+1,bq+c}$  where  $\gamma = a+1$ ,  $\alpha = c-1$  and  $\beta = b+1$ . By doing this,  $c$  becomes the block index and  $a, b$  become the position in the dense block. This mapping can be represented by left and right permutation matrices which also prescribe the permutation for the rest of the elements of  $M$ . A graphical sketch of this coordinate permutation is shown in Figure 4.  $\square$

## 5 Numerical Experiments

In this section, we compare state evolution predictions from Theorem 4.2 with a numerical implementation of the ML-AMP algorithm described in Section 3.3.

Our first experiment, shown in Figure 1, is a noisy compressive sensing task under a sparsity prior  $P_X(x) = \rho \mathcal{N}(x; 0, 1) + (1 - \rho)\delta(x)$ , where  $\rho$  is the expected fraction of nonzero components of  $x_0$ . Measurements are generated  $y_0 = Wx_0 + \eta$  for noise  $\eta \sim \mathcal{N}(0, 10^{-4})$ , where  $W \sim \text{MCC}(D, P, q, k)$ . We show recovery performance at sparsity levels  $\rho \in \{0.25, 0.5, 0.75\}$  as the measurement ratio  $\beta = D/P$  varies, averaged over 10 independent AMP iterates. Additionally, we show convergence of the (averaged) AMP iterates for sparsity  $\rho = 0.25$  at a range of  $\beta$  near the recovery threshold. We observe strong agreement between AMP empirical performance and the state evolution prediction. The system sizes are  $P = 1024$ ,  $q = 1024$ , with  $D = \beta P$  varying.

In Figure 5, we show two examples of  $L = 2, 3, 4$  layer models following Equation (2). In both, the output channel  $l = 1$  generates noisy, compressive linear measurements  $y = z^{(1)} + \zeta$  for  $\zeta_i \sim \mathcal{N}(0, \sigma^2)$  and for dense couplings  $W_{ij}^{(1)} \sim \mathcal{N}(0, 1/n^{(1)})$ . Layers  $2 \leq l \leq 4$  use MCC couplings  $W^{(l)} \sim \text{MCC}(D_l, P_l, q, k)$ , where  $qP_l = n_l$  and  $D_l = \beta P_l = qn_{l-1}$ . Channel functions  $\{\varphi^{(l)}\}$  vary across the two experiments. The input prior is  $P_X(x) = \mathcal{N}(x; 0, 1)$  and model has  $q = 10$  channels, filter size  $k = 3$ , noise level  $\sigma^2 = 10^{-4}$ , input dimension  $n^{(L)} = 5000$ , layerwise aspect ratios  $\beta^{(L)} = 2$  and  $\beta^{(l)} = 1$  for  $2 \leq l < L$ . The channel aspect ratio  $\beta^{(1)}$  varies in each experiment.

We compare the state evolution equations to empirical AMP results in two cases. In the left panel, we show multilayer models with identity channel functions, and in the right panel, we show models with ReLU channel functions. The latter model captures a simple but accurate example of a convolutional generative neural network.

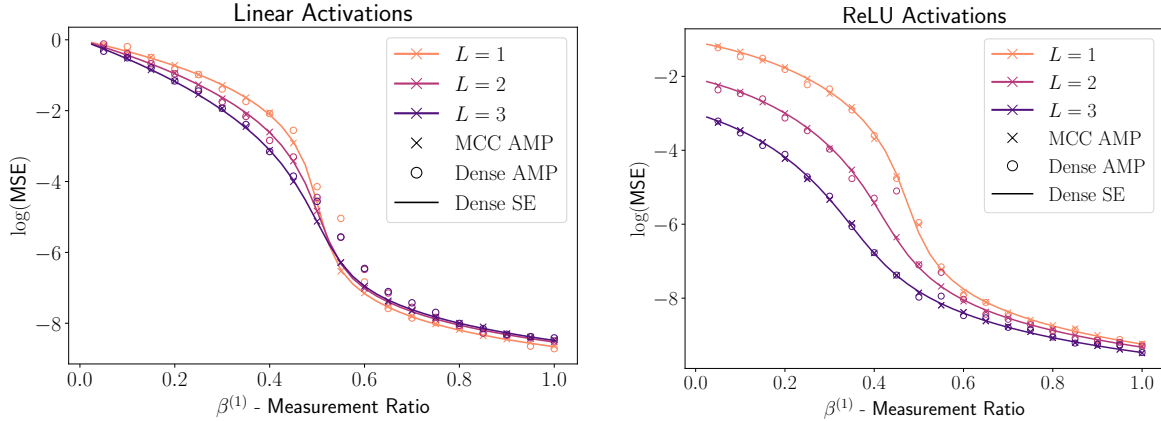


Figure 5: ML-AMP compressive sensing recovery under multichannel convolutional designs (crossed) and the state evolution for the corresponding fully connected model (lined). For comparison, we also plot the corresponding fully connected AMP iterations (dotted), in which  $W^{(l)} \in \mathbb{R}^{D_l \times P_l}$  with  $W_{ij} \sim \mathcal{N}(0, 1/P_l)$ , with the dimensions of the prior and output channel adjusted appropriately. Left: For  $2 \leq l \leq L$ , the channel functions are  $\varphi^{(l)}(z; \zeta) = z + \zeta$  where  $\zeta_i \sim \mathcal{N}(0, \sigma^2)$ . Right: For  $2 \leq l \leq L$ , the channel functions are  $\varphi^{(l)}(z; \zeta) = \max(z, 0)$  where the maximum is applied coordinatewise. This channel function is the popular ReLU activation function used by generative convolutional neural networks such as in [Radford et al., 2015; Bora et al., 2017].

## 6 Discussion and Future Work

We have proven state evolution recursions for the ML-AMP algorithm for signal recovery from multi-layer convolutional networks. We consider networks whose weight matrices are drawn either i.i.d. Gaussian or from an ensemble of random multi-channel convolution matrices. Interestingly, under a separable prior and separable channel functions, these two matrix ensembles yield the same state evolution (up to a rescaling). These predictions closely match empirical observations in compressive sensing under a sparsity prior (Figure 1) and under multi-layer priors (Figure 5).

Lemma (4.3) allows to rewrite an MCC matrix  $M$  as a block circulant matrix  $\tilde{M}$  with random extensive blocks, reminiscent of the block structure of spatially coupled sensing matrices. As a consequence of separability, the nonzero blocks of  $\tilde{M}$  have identical statistics, which is key to our equivalence theorem between MCC matrices and their dense i.i.d. counterparts. This is in contrast to spatial coupling, where extensive blocks may have different variances, or equivalently when denoising functions may be non-separable. We prove in Appendix A a more general result for non-separable channel functions, of which Theorem 4.2 is a specialization to the separable case. In Appendix D, we discuss a potential application to signal recovery with non-i.i.d. convolutional filters, in which the dynamics of ML-AMP is expected to differ from the analogous fully connected model. Ultimately, studying non-separable models is an interesting and potentially fruitful avenue for future work.

Another important direction for future work is to go beyond random convolutional layers and study how to account for trained layers in the ML-AMP algorithm and its state evolution.

## Acknowledgments and Disclosure of Funding

M.D. acknowledges funding from Northeastern University’s Undergraduate Research & Fellowships office and the Goldwater Award. We acknowledge funding from the ERC under the European Union’s Horizon 2020 Research and Innovation Program Grant Agreement 714608-SMiLe.

## References

- Muhammad Asim, Max Daniels, Oscar Leong, Ali Ahmed, and Paul Hand. Invertible generative models for inverse problems: mitigating representation error and dataset bias. In Hal Daumé III and Aarti Singh, editors, *Proceedings of the 37th International Conference on Machine Learning*, volume 119 of *Proceedings of Machine Learning Research*, pages 399–409. PMLR, 13–18 Jul 2020. URL <https://proceedings.mlr.press/v119/asim20a.html>.
- Benjamin Aubin, Bruno Loureiro, Antoine Maillard, Florent Krzakala, and Lenka Zdeborová. The spiked matrix model with generative priors. *Advances in Neural Information Processing Systems*, 32, 2019.
- Antoine Baker, Benjamin Aubin, Florent Krzakala, and Lenka Zdeborová. Tramp: Compositional inference with tree approximate message passing. *arXiv preprint arXiv:2004.01571*, 2020.
- Jean Barbier, Christophe Schülke, and Florent Krzakala. Approximate message-passing with spatially coupled structured operators, with applications to compressed sensing and sparse superposition codes. *Journal of Statistical Mechanics: Theory and Experiment*, 2015(5):P05013, 2015.
- Mohsen Bayati and Andrea Montanari. The dynamics of message passing on dense graphs, with applications to compressed sensing. *IEEE Transactions on Information Theory*, 57(2):764–785, 2011.
- Raphael Berthier, Andrea Montanari, and Phan-Minh Nguyen. State evolution for approximate message passing with non-separable functions. *Information and Inference: A Journal of the IMA*, 9(1):33–79, 2020.
- Erwin Bolthausen. On the high-temperature phase of the sherrington-kirkpatrick model, Sep 2009.
- Ashish Bora, Ajil Jalal, Eric Price, and Alexandros G Dimakis. Compressed sensing using generative models. In *International Conference on Machine Learning*, pages 537–546. PMLR, 2017.
- Giannis Daras, Joseph Dean, Ajil Jalal, and Alex Dimakis. Intermediate layer optimization for inverse problems using deep generative models. In Marina Meila and Tong Zhang, editors, *Proceedings of the 38th International Conference on Machine Learning*, volume 139 of *Proceedings of Machine Learning Research*, pages 2421–2432. PMLR, 18–24 Jul 2021. URL <https://proceedings.mlr.press/v139/daras21a.html>.
- David L Donoho, Arian Maleki, and Andrea Montanari. Message-passing algorithms for compressed sensing. *Proceedings of the National Academy of Sciences*, 106(45):18914–18919, 2009.
- David L Donoho, Adel Javanmard, and Andrea Montanari. Information-theoretically optimal compressed sensing via spatial coupling and approximate message passing. *IEEE transactions on information theory*, 59(11):7434–7464, 2013.
- A Jimenez Felstrom and Kamil Sh Zigangirov. Time-varying periodic convolutional codes with low-density parity-check matrix. *IEEE Transactions on Information Theory*, 45(6):2181–2191, 1999.
- Alyson K Fletcher, Sundeep Rangan, and Philip Schniter. Inference in deep networks in high dimensions. In *2018 IEEE International Symposium on Information Theory (ISIT)*, pages 1884–1888. IEEE, 2018.
- Cédric Gerbelot and Raphaël Berthier. Graph-based approximate message passing iterations. *arXiv preprint arXiv:2109.11905*, 2021.
- Rafael C. Gonzalez and Richard E. Woods. *Digital image processing, 3rd Edition*. Pearson Education, 2008. ISBN 9780135052679. URL <https://www.worldcat.org/oclc/241057034>.
- Jinjin Gu, Yujun Shen, and Bolei Zhou. Image processing using multi-code gan prior. In *CVPR*, 2020.

- Ajil Jalal, Sushrut Karmalkar, Alex Dimakis, and Eric Price. Instance-optimal compressed sensing via posterior sampling. In Marina Meila and Tong Zhang, editors, *Proceedings of the 38th International Conference on Machine Learning*, volume 139 of *Proceedings of Machine Learning Research*, pages 4709–4720. PMLR, 18–24 Jul 2021. URL <https://proceedings.mlr.press/v139/jalal21a.html>.
- Adel Javanmard and Andrea Montanari. State evolution for general approximate message passing algorithms, with applications to spatial coupling. *Information and Inference: A Journal of the IMA*, 2(2):115–144, 2013.
- Tero Karras, Timo Aila, Samuli Laine, and Jaakko Lehtinen. Progressive growing of GANs for improved quality, stability, and variation. In *International Conference on Learning Representations*, 2018. URL <https://openreview.net/forum?id=Hk99zCeAb>.
- Tero Karras, Samuli Laine, and Timo Aila. A style-based generator architecture for generative adversarial networks. In *Proceedings of the IEEE/CVF conference on computer vision and pattern recognition*, pages 4401–4410, 2019.
- Durk P Kingma and Prafulla Dhariwal. Glow: Generative flow with invertible 1x1 convolutions. In S. Bengio, H. Wallach, H. Larochelle, K. Grauman, N. Cesa-Bianchi, and R. Garnett, editors, *Advances in Neural Information Processing Systems*, volume 31. Curran Associates, Inc., 2018. URL <https://proceedings.neurips.cc/paper/2018/file/d139db6a236200b21cc7f752979132d0-Paper.pdf>.
- Alex Krizhevsky, Ilya Sutskever, and Geoffrey E Hinton. Imagenet classification with deep convolutional neural networks. *Advances in neural information processing systems*, 25, 2012.
- Florent Krzakala, Marc Mézard, François Sausset, YF Sun, and Lenka Zdeborová. Statistical-physics-based reconstruction in compressed sensing. *Physical Review X*, 2(2):021005, 2012.
- Shrinivas Kudekar, Thomas J Richardson, and Rüdiger L Urbanke. Threshold saturation via spatial coupling: Why convolutional ldpc ensembles perform so well over the bec. *IEEE Transactions on Information Theory*, 57(2):803–834, 2011.
- Shrinivas Kudekar, Tom Richardson, and Rüdiger L Urbanke. Spatially coupled ensembles universally achieve capacity under belief propagation. *IEEE Transactions on Information Theory*, 59(12):7761–7813, 2013.
- Andre Manoel, Florent Krzakala, Marc Mézard, and Lenka Zdeborová. Multi-layer generalized linear estimation. In *2017 IEEE International Symposium on Information Theory (ISIT)*, pages 2098–2102. IEEE, 2017.
- Christopher A Metzler, Arian Maleki, and Richard G Baraniuk. Bm3d-amp: A new image recovery algorithm based on bm3d denoising. In *2015 IEEE International Conference on Image Processing (ICIP)*, pages 3116–3120. IEEE, 2015.
- Marc Mézard and Andrea Montanari. *Information, physics, and computation*. Oxford University Press, 2009.
- Alec Radford, Luke Metz, and Soumith Chintala. Unsupervised representation learning with deep convolutional generative adversarial networks. *arXiv preprint arXiv:1511.06434*, 2015.
- Sundeeep Rangan. Generalized approximate message passing for estimation with random linear mixing. In *2011 IEEE International Symposium on Information Theory Proceedings*, pages 2168–2172. IEEE, 2011.

- Sundeeep Rangan and Alyson K Fletcher. Iterative estimation of constrained rank-one matrices in noise. In *2012 IEEE International Symposium on Information Theory Proceedings*, pages 1246–1250. IEEE, 2012.
- Sundeeep Rangan, Philip Schniter, and Alyson K Fletcher. Vector approximate message passing. *IEEE Transactions on Information Theory*, 65(10):6664–6684, 2019.
- Philip Schniter, Sundeeep Rangan, and Alyson K Fletcher. Vector approximate message passing for the generalized linear model. In *2016 50th Asilomar Conference on Signals, Systems and Computers*, pages 1525–1529. IEEE, 2016.
- Yang Song and Stefano Ermon. Improved techniques for training score-based generative models. In Hugo Larochelle, Marc’ Aurelio Ranzato, Raia Hadsell, Maria-Florina Balcan, and Hsuan-Tien Lin, editors, *Advances in Neural Information Processing Systems 33: Annual Conference on Neural Information Processing Systems 2020, NeurIPS 2020, December 6-12, 2020, virtual*, 2020.
- Lenka Zdeborová and Florent Krzakala. Statistical physics of inference: Thresholds and algorithms. *Advances in Physics*, 65(5):453–552, 2016.
- Matthew D Zeiler and Rob Fergus. Visualizing and understanding convolutional networks. In *European conference on computer vision*, pages 818–833. Springer, 2014.

## A Proof of the main theorem

The proof of the main theorem is presented in this section. We start with a generic result on a family of AMP iterations including the (non Bayes-optimal) MLAMP one, using the framework of [Gerbelot and Berthier, 2021], from which we remind the required notions.

### A.1 Notations and definitions

If  $f : \mathbb{R}^{N \times q} \rightarrow \mathbb{R}^{N \times q}$  is a function and  $i \in \{1, \dots, N\}$ , we write  $f_i : \mathbb{R}^{N \times q} \rightarrow \mathbb{R}^q$  the component of  $f$  generating the  $i$ -th line of its image, i.e., if  $\mathbf{X} \in \mathbb{R}^{N \times q}$ ,

$$f(\mathbf{X}) = \begin{bmatrix} f_1(\mathbf{X}) \\ \vdots \\ f_N(\mathbf{X}) \end{bmatrix} \in \mathbb{R}^{N \times q}.$$

We write  $\frac{\partial f_i}{\partial \mathbf{X}_i}$  the  $q \times q$  Jacobian containing the derivatives of  $f_i$  with respect to (w.r.t.) the  $i$ -th line  $\mathbf{X}_i \in \mathbb{R}^q$ :

$$\frac{\partial f_i}{\partial \mathbf{X}_i} = \begin{bmatrix} \frac{\partial (f_i(\mathbf{X}))_1}{\partial \mathbf{X}_{i1}} & \cdots & \frac{\partial (f_i(\mathbf{X}))_1}{\partial \mathbf{X}_{iq}} \\ \vdots & & \vdots \\ \frac{\partial (f_i(\mathbf{X}))_q}{\partial \mathbf{X}_{i1}} & \cdots & \frac{\partial (f_i(\mathbf{X}))_q}{\partial \mathbf{X}_{iq}} \end{bmatrix} \in \mathbb{R}^{q \times q}. \quad (9)$$

For two sequences of random variables  $X_n, Y_n$ , we write  $X_n \stackrel{P}{\simeq} Y_n$  when their difference converges in probability to 0, i.e.,  $X_n - Y_n \xrightarrow{P} 0$ . Oriented graphs with a set of vertices  $V$  and edges  $\vec{E}$  are denoted  $G = (V, \vec{E})$ . The set of edges may be split into right-pointing and left-pointing edges, i.e.,  $\vec{E} = \{\vec{e}_1, \dots, \vec{e}_L\}$ ,  $\overleftarrow{E} = \{\overleftarrow{e}_1, \dots, \overleftarrow{e}_L\}$ .

**Definition A.1** (pseudo-Lipschitz function). For  $k \in \mathbb{N}^*$  and any  $N, m \in \mathbb{N}^*$ , a function  $\Phi : \mathbb{R}^{N \times q} \rightarrow \mathbb{R}^{m \times q}$  is said to be *pseudo-Lipschitz of order  $k$*  if there exists a constant  $L$  such that for any  $\mathbf{x}, \mathbf{y} \in \mathbb{R}^{N \times q}$ ,

$$\frac{\|\Phi(\mathbf{x}) - \Phi(\mathbf{y})\|_F}{\sqrt{m}} \leq L \left( 1 + \left( \frac{\|\mathbf{x}\|_F}{\sqrt{N}} \right)^{k-1} + \left( \frac{\|\mathbf{y}\|_F}{\sqrt{N}} \right)^{k-1} \right) \frac{\|\mathbf{x} - \mathbf{y}\|_F}{\sqrt{N}} \quad (10)$$

For a function  $\varphi : \mathbb{R} \rightarrow \mathbb{R}$ , the property becomes

$$\forall (x, y) \in \mathbb{R}^2, |\varphi(x) - \varphi(y)| \leq L(1 + |x|^{k-1} + |y|^{k-1})|x - y| \quad (11)$$

and a straightforward calculation shows that for any scalar pseudo-Lipschitz function of order 2, the function

$$\phi : \mathbb{R}^d \rightarrow \mathbb{R}, \quad (12)$$

$$\mathbf{x} \mapsto \frac{1}{d} \sum_{i=1}^d \varphi(x_i) \quad (13)$$

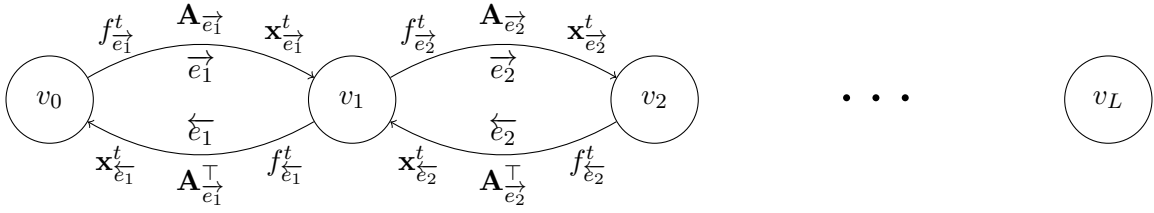
is pseudo-Lipschitz of order 2 according to the definition above. This definition is handy for proofs involving non-separable functions and leads to Gaussian concentration using the Gauss-Poincaré inequality (see Lemma C.8. from [Berthier et al., 2020]), while in the separable case, a strong law of large number is proven for a class of distributions including sub-Gaussian ones in Lemma 5 of [Bayati and Montanari, 2011].

## A.2 State evolution for generic multilayer AMP iterations with matrix valued variables and dense Gaussian matrices

In the notations of [Gerbelot and Berthier, 2021], consider the AMP iteration indexed by the following directed graph  $G = (V, \vec{E})$ , where the set of vertices is denoted  $V = \{v_0, v_1, \dots, v_L\}$ , and the set of edges  $\vec{E} = \{\vec{e}_1, \dots, \vec{e}_L, \overleftarrow{e}_1, \dots, \overleftarrow{e}_L\}$ . For any edge  $\vec{e}_l$ , the corresponding matrix  $\mathbf{A}_{\vec{e}_l}$  has dimensions  $\mathbb{R}^{n_l \times n_{l-1}}$  with  $\mathbf{A}_{\overleftarrow{e}_l} = \mathbf{A}_{\vec{e}_l}^\top$ , and the variables  $\mathbf{x}_{\vec{e}_l} \in \mathbb{R}^{n_l \times q}$ ,  $\mathbf{x}_{\overleftarrow{e}_l} \in \mathbb{R}^{n_{l-1} \times q}$  for some finite  $q \in \mathbb{N}$ , with  $N = \sum_{l=1}^L n_l$ . Finally, we define the non-linearities of the iteration by specifying the variables they are acting on as follows:

- $f_{\vec{e}_1}^t : \mathbb{R}^{n_0 \times q} \rightarrow \mathbb{R}^{n_0 \times q}$ ,  $\mathbf{x}_{\overleftarrow{e}_1}^t \mapsto f_{\vec{e}_1}^t(\mathbf{x}_{\overleftarrow{e}_1}^t)$ ,
- for any  $2 \leq l \leq L$ ,  $f_{\vec{e}_l}^t : (\mathbb{R}^{n_{l-1} \times q})^2 \rightarrow \mathbb{R}^{n_{l-1} \times q}$ ,  $(\mathbf{x}_{\vec{e}_{l-1}}^t, \mathbf{x}_{\overleftarrow{e}_l}^t) \mapsto f_{\vec{e}_l}^t(\mathbf{x}_{\vec{e}_{l-1}}^t, \mathbf{x}_{\overleftarrow{e}_l}^t)$ ,
- for any  $1 \leq l \leq L-1$ ,  $f_{\overleftarrow{e}_l}^t : (\mathbb{R}^{n_l \times q})^3 \rightarrow \mathbb{R}^{n_l \times q}$ ,  $(\mathbf{x}_{\vec{e}_l}^t, \mathbf{x}_{\overleftarrow{e}_{l+1}}^t) \mapsto f_{\overleftarrow{e}_l}^t(\mathbf{A}_{\vec{e}_l} \mathbf{w}_{\vec{e}_l}, \mathbf{x}_{\vec{e}_l}^t, \mathbf{x}_{\overleftarrow{e}_{l+1}}^t)$
- $f_{\overleftarrow{e}_L}^t : (\mathbb{R}^{n_L \times q})^2 \rightarrow \mathbb{R}^{n_L \times q}$ ,  $\mathbf{x}_{\vec{e}_L}^t \mapsto f_{\overleftarrow{e}_L}^t(\mathbf{A}_{\overleftarrow{e}_L} \mathbf{w}_{\overleftarrow{e}_L}, \mathbf{x}_{\vec{e}_L}^t)$

where  $\mathbf{w}_{\vec{e}_1}, \dots, \mathbf{w}_{\overleftarrow{e}_L}$  are low-rank matrices respectively in  $\mathbb{R}^{n_0 \times q}, \dots, \mathbb{R}^{n_{L-1} \times q}$ , whose rows are sampled i.i.d. from subgaussian probability distributions in  $\mathbb{R}^q$ . The graph indexing the iteration then reads:



with the corresponding iteration:

$$\begin{aligned}
\mathbf{x}_{\vec{e}_1}^{t+1} &= \mathbf{A}_{\vec{e}_1} \mathbf{m}_{\vec{e}_1}^t - \mathbf{m}_{\vec{e}_1}^{t-1} \left( \mathbf{b}_{\vec{e}_1}^t \right)^\top, \\
\mathbf{m}_{\vec{e}_1}^t &= f_{\vec{e}_1}^t \left( \mathbf{x}_{\vec{e}_1}^t \right), \\
\mathbf{x}_{\overleftarrow{e}_1}^{t+1} &= \mathbf{A}_{\overleftarrow{e}_1}^\top \mathbf{m}_{\overleftarrow{e}_1}^t - \mathbf{m}_{\overleftarrow{e}_1}^{t-1} \left( \mathbf{b}_{\overleftarrow{e}_1}^t \right)^\top, \\
\mathbf{m}_{\overleftarrow{e}_1}^t &= f_{\overleftarrow{e}_1}^t \left( \mathbf{A}_{\overleftarrow{e}_1} \mathbf{w}_{\overleftarrow{e}_1}, \mathbf{x}_{\overleftarrow{e}_1}^t, \mathbf{x}_{\overleftarrow{e}_2}^t \right), \\
\\
\mathbf{x}_{\vec{e}_2}^{t+1} &= \mathbf{A}_{\vec{e}_2} \mathbf{m}_{\vec{e}_2}^t - \mathbf{m}_{\vec{e}_2}^{t-1} \left( \mathbf{b}_{\vec{e}_2}^t \right)^\top, \\
\mathbf{m}_{\vec{e}_2}^t &= f_{\vec{e}_2}^t \left( \mathbf{x}_{\vec{e}_1}^t, \mathbf{x}_{\vec{e}_2}^t \right), \\
\mathbf{x}_{\overleftarrow{e}_2}^{t+1} &= \mathbf{A}_{\overleftarrow{e}_2}^\top \mathbf{m}_{\overleftarrow{e}_2}^t - \mathbf{m}_{\overleftarrow{e}_2}^{t-1} \left( \mathbf{b}_{\overleftarrow{e}_2}^t \right)^\top, \\
\mathbf{m}_{\overleftarrow{e}_2}^t &= f_{\overleftarrow{e}_2}^t \left( \mathbf{A}_{\overleftarrow{e}_2} \mathbf{w}_{\overleftarrow{e}_2}, \mathbf{x}_{\overleftarrow{e}_2}^t, \mathbf{x}_{\overleftarrow{e}_3}^t \right), \\
\\
&\vdots \\
\\
\mathbf{x}_{\vec{e}_L}^{t+1} &= \mathbf{A}_{\vec{e}_L} \mathbf{m}_{\vec{e}_L}^t - \mathbf{m}_{\vec{e}_L}^{t-1} \left( \mathbf{b}_{\vec{e}_L}^t \right)^\top, \\
\mathbf{m}_{\vec{e}_L}^t &= f_{\vec{e}_L}^t \left( \mathbf{x}_{\vec{e}_{L-1}}^t, \mathbf{x}_{\vec{e}_L}^t \right), \\
\mathbf{x}_{\overleftarrow{e}_L}^{t+1} &= \mathbf{A}_{\overleftarrow{e}_L}^\top \mathbf{m}_{\overleftarrow{e}_L}^t - \mathbf{m}_{\overleftarrow{e}_L}^{t-1} \left( \mathbf{b}_{\overleftarrow{e}_L}^t \right)^\top, \\
\mathbf{m}_{\overleftarrow{e}_L}^t &= f_{\overleftarrow{e}_L}^t \left( \mathbf{A}_{\overleftarrow{e}_L} \mathbf{w}_{\overleftarrow{e}_L}, \mathbf{x}_{\overleftarrow{e}_L}^t \right)
\end{aligned} \tag{14}$$

and Onsager terms, for the right oriented edges

$$\mathbf{b}_{\vec{e}_l}^t = \frac{1}{N} \sum_{i=1}^{n_{l-1}} \frac{\partial f_{\vec{e}_l, i}^t}{\partial \mathbf{x}_{\vec{e}_l, i}} \left( \left( \mathbf{x}_{\vec{e}'_l}^t \right)_{\vec{e}'_l: \vec{e}'_l \rightarrow \vec{e}_l} \right) \in \mathbb{R}^{q \times q}.$$

and left oriented edges

$$\mathbf{b}_{\overleftarrow{e}_l}^t = \frac{1}{N} \sum_{i=1}^{n_l} \frac{\partial f_{\overleftarrow{e}_l, i}^t}{\partial \mathbf{x}_{\overleftarrow{e}_l, i}} \left( \mathbf{A}_{\overleftarrow{e}_l} \mathbf{w}_{\overleftarrow{e}_l}, \left( \mathbf{x}_{\overleftarrow{e}'_l}^t \right)_{\overleftarrow{e}'_l: \overleftarrow{e}'_l \rightarrow \overleftarrow{e}_l} \right) \in \mathbb{R}^{q \times q}.$$

We now make the following assumptions

- (A1) The matrices  $(\mathbf{A}_{\vec{e}})_{\vec{e} \in \vec{E}}$  are random and independent, up to the symmetry condition  $\mathbf{A}_{\overleftarrow{e}} = \mathbf{A}_{\vec{e}}^\top$ . Moreover  $\mathbf{A}_{\vec{e}}$  has independent centered Gaussian entries with variance  $1/N$ .
- (A2) For all  $1 \leq l \leq L$ ,  $n_l \rightarrow \infty$  and  $n_l/N$  converges to a well-defined limit  $\delta_l \in [0, 1]$ . We denote by  $n \rightarrow \infty$  the limit under this scaling.
- (A3) For all  $t \in \mathbb{N}$  and  $\vec{e} \in \vec{E}$ , the non-linearity  $f_{\vec{e}}^t$  is pseudo-Lipschitz of finite order, uniformly with respect to the problem dimensions  $(n_l)_{0 \leq l \leq L}$ .
- (A4) For all  $\vec{e} \in E$ , the lines of  $\mathbf{x}_{\vec{e}}^0$ ,  $\mathbf{w}_{\vec{e}}$  are sampled from subgaussian probability distributions in  $\mathbf{R}^q$ .
- (A5) For all  $\vec{e} \in E$ , the following limit exists and is finite:

$$\lim_{n \rightarrow \infty} \frac{1}{N} \left\langle f_{\vec{e}}^0 \left( \left( \mathbf{x}_{\vec{e}'_l}^0 \right)_{\vec{e}'_l: \vec{e}'_l \rightarrow \vec{e}} \right), f_{\vec{e}}^0 \left( \left( \mathbf{x}_{\vec{e}'_l}^0 \right)_{\vec{e}'_l: \vec{e}'_l \rightarrow \vec{e}} \right) \right\rangle$$



(A6) Let  $(\kappa_{\vec{e}})_{\vec{e} \in E}$  be an array of bounded non-negative reals and  $\mathbf{Z}_{\vec{e}} \sim \mathbf{N}(0, \kappa_{\vec{e}} \mathbf{I}_{n_w})$  independent random variables for all  $\vec{e}$ . For all  $\vec{e} \in E$ , for any  $t \in \mathbb{N}_{>0}$ , the following limit exists and is finite:

$$\lim_{n \rightarrow \infty} \frac{1}{N} \mathbb{E} \left[ \left\langle f_{\vec{e}}^0 \left( (\mathbf{x}_{\vec{e}'}^0)_{\vec{e}': \vec{e}' \rightarrow \vec{e}} \right), f_{\vec{e}}^t \left( (\mathbf{Z}_{\vec{e}'}^t)_{\vec{e}': \vec{e}' \rightarrow \vec{e}} \right) \right\rangle \right].$$

(A7) Consider any array of  $2 \times 2$  positive definite matrices  $(\mathbf{S}_{\vec{e}})_{\vec{e} \in E}$  and the collection of random variables  $(\mathbf{Z}_{\vec{e}}, \mathbf{Z}'_{\vec{e}}) \sim \mathbf{N}(0, \mathbf{S}_{\vec{e}} \otimes \mathbf{I}_{n_w})$  defined independently for each edge  $\vec{e}$ . Then for any  $\vec{e} \in E$  and  $s, t > 0$ , the following limit exists and is finite:

$$\lim_{n \rightarrow \infty} \frac{1}{N} \mathbb{E} \left[ \left\langle f_{\vec{e}}^s \left( (\mathbf{Z}_{\vec{e}'}^s)_{\vec{e}': \vec{e}' \rightarrow \vec{e}} \right), f_{\vec{e}}^t \left( (\tilde{\mathbf{Z}}_{\vec{e}'}^t)_{\vec{e}': \vec{e}' \rightarrow \vec{e}} \right) \right\rangle \right].$$

Under these assumptions, we define the following state evolution recursion:

• for  $l = 1$  :

$$\boldsymbol{\nu}_{\vec{e}_1}^0 = \lim_{N \rightarrow \infty} \frac{1}{N} \mathbf{w}_{\vec{e}_1}^\top f_{\vec{e}_1}^0(\mathbf{x}_{\vec{e}_1}^0), \quad \boldsymbol{\kappa}_{\vec{e}_1}^{1,1} = \lim_{N \rightarrow \infty} \frac{1}{N} f_{\vec{e}_1}^0(\mathbf{x}_{\vec{e}_1}^0)^\top f_{\vec{e}_1}^0(\mathbf{x}_{\vec{e}_1}^0) \quad (15)$$

$$\boldsymbol{\nu}_{\vec{e}_1}^{t+1} = \lim_{N \rightarrow +\infty} \frac{1}{N} \mathbb{E} \left[ \mathbf{w}_{\vec{e}_1}^\top f_{\vec{e}_1}^t \left( \mathbf{w}_{\vec{e}_1} \hat{\boldsymbol{\nu}}_{\vec{e}_1}^t + \mathbf{Z}_{\vec{e}_1}^t \right) \right] \quad (16)$$

$$\begin{aligned} \boldsymbol{\kappa}_{\vec{e}_1}^{s+1, t+1} = \boldsymbol{\kappa}_{\vec{e}_1}^{t+1, s+1} &= \lim_{N \rightarrow +\infty} \frac{1}{N} \mathbb{E} \left[ \left( f_{\vec{e}_1}^s \left( \mathbf{w}_{\vec{e}_1} \hat{\boldsymbol{\nu}}_{\vec{e}_1}^s + \mathbf{Z}_{\vec{e}_1}^s \right) - \mathbf{w}_{\vec{e}_1} \rho_{\mathbf{w}_{\vec{e}_1}}^{-1} \boldsymbol{\nu}_{\vec{e}_1}^{s+1} \right)^\top \right. \\ &\left. \left( f_{\vec{e}_1}^t \left( \mathbf{w}_{\vec{e}_1} \hat{\boldsymbol{\nu}}_{\vec{e}_1}^t + \mathbf{Z}_{\vec{e}_1}^t \right) - \mathbf{w}_{\vec{e}_1} \rho_{\mathbf{w}_{\vec{e}_1}}^{-1} \boldsymbol{\nu}_{\vec{e}_1}^{t+1} \right) \right] \quad (17) \end{aligned}$$

$$\hat{\boldsymbol{\nu}}_{\vec{e}_1}^0, \boldsymbol{\kappa}_{\vec{e}_1}^{1,1} = \lim_{n \rightarrow \infty} \frac{1}{N} f_{\vec{e}_1}^0 \left( \mathbf{z}_{\mathbf{w}_{\vec{e}_1}}, \mathbf{x}_{\vec{e}_1}^0, \mathbf{x}_{\vec{e}_2}^0 \right)^\top f_{\vec{e}_1}^0 \left( \mathbf{z}_{\mathbf{w}_{\vec{e}_1}}, \mathbf{x}_{\vec{e}_1}^0, \mathbf{x}_{\vec{e}_2}^0 \right) \quad (18)$$

$$\hat{\boldsymbol{\nu}}_{\vec{e}_1}^{t+1} = \lim_{N \rightarrow \infty} \frac{1}{N} \mathbb{E} \left[ \sum_{i=1}^N \frac{\partial f_{\vec{e}_1}^t}{\partial \mathbf{z}_{\mathbf{w}_{\vec{e}_1}, i}, \phi_{\vec{e}_1}^t} \left( \mathbf{z}_{\mathbf{w}_{\vec{e}_1}}, \mathbf{z}_{\mathbf{w}_{\vec{e}_1}} \rho_{\mathbf{w}_{\vec{e}_1}}^{-1} \boldsymbol{\nu}_{\vec{e}_1}^t + \mathbf{Z}_{\vec{e}_1}^t, \mathbf{w}_{\vec{e}_2} \hat{\boldsymbol{\nu}}_{\vec{e}_2}^t + \mathbf{Z}_{\vec{e}_2}^t \right) \right] \quad (19)$$

$$\begin{aligned} \boldsymbol{\kappa}_{\vec{e}_1}^{s+1, t+1} &= \lim_{n \rightarrow \infty} \frac{1}{N} \mathbb{E} \left[ f_{\vec{e}_1}^s \left( \mathbf{z}_{\mathbf{w}_{\vec{e}_1}}, \mathbf{z}_{\mathbf{w}_{\vec{e}_1}} \rho_{\mathbf{w}_{\vec{e}_1}}^{-1} \boldsymbol{\nu}_{\vec{e}_1}^s + \mathbf{Z}_{\vec{e}_1}^s, \mathbf{w}_{\vec{e}_2} \hat{\boldsymbol{\nu}}_{\vec{e}_2}^s + \mathbf{Z}_{\vec{e}_2}^s \right)^\top \right. \\ &\left. f_{\vec{e}_1}^t \left( \mathbf{z}_{\mathbf{w}_{\vec{e}_1}}, \mathbf{z}_{\mathbf{w}_{\vec{e}_1}} \rho_{\mathbf{w}_{\vec{e}_1}}^{-1} \boldsymbol{\nu}_{\vec{e}_1}^t + \mathbf{Z}_{\vec{e}_1}^t, \mathbf{w}_{\vec{e}_2} \hat{\boldsymbol{\nu}}_{\vec{e}_2}^t + \mathbf{Z}_{\vec{e}_2}^t \right) \right] \quad (20) \end{aligned}$$

- for any  $2 \leq l \leq L-1$

$$\boldsymbol{\nu}_{\leftarrow e_l}^0 = \lim_{N \rightarrow \infty} \frac{1}{N} \mathbf{w}_{\leftarrow e_l}^\top f_{\leftarrow e_l}^0(\mathbf{x}_{\leftarrow e_l}^0), \boldsymbol{\kappa}_{\leftarrow e_l}^{1,1} = \lim_{N \rightarrow \infty} \frac{1}{N} f_{\leftarrow e_l}^0(\mathbf{x}_{\leftarrow e_l}^0)^\top f_{\leftarrow e_l}^0(\mathbf{x}_{\leftarrow e_l}^0) \quad (21)$$

$$\boldsymbol{\nu}_{\leftarrow e_l}^{t+1} = \lim_{N \rightarrow +\infty} \frac{1}{N} \mathbb{E} \left[ \mathbf{w}_{\leftarrow e_l}^\top f_{\leftarrow e_l}^t \left( \mathbf{z}_{\mathbf{w}_{\leftarrow e_{l-1}}} \rho_{\mathbf{w}_{\leftarrow e_{l-1}}}^{-1} \boldsymbol{\nu}_{\leftarrow e_{l-1}}^t + \mathbf{Z}_{\leftarrow e_{l-1}}^t, \mathbf{w}_{\leftarrow e_l} \hat{\boldsymbol{\nu}}_{\leftarrow e_l}^t + \mathbf{Z}_{\leftarrow e_l}^t \right) \right] \quad (22)$$

$$\boldsymbol{\kappa}_{\leftarrow e_l}^{s+1,t+1} = \boldsymbol{\kappa}_{\leftarrow e_l}^{t+1,s+1} = \lim_{N \rightarrow +\infty} \quad (23)$$

$$\frac{1}{N} \mathbb{E} \left[ \left( f_{\leftarrow e_l}^s \left( \mathbf{z}_{\mathbf{w}_{\leftarrow e_{l-1}}} \rho_{\mathbf{w}_{\leftarrow e_{l-1}}}^{-1} \boldsymbol{\nu}_{\leftarrow e_{l-1}}^s + \mathbf{Z}_{\leftarrow e_{l-1}}^s, \mathbf{w}_{\leftarrow e_l} \hat{\boldsymbol{\nu}}_{\leftarrow e_l}^s + \mathbf{Z}_{\leftarrow e_l}^s \right) - \mathbf{w}_{\leftarrow e_l} \rho_{\mathbf{w}_{\leftarrow e_l}}^{-1} \boldsymbol{\nu}_{\leftarrow e_l}^{s+1} \right)^\top \right. \right. \\ \left. \left. \left( f_{\leftarrow e_l}^t \left( \mathbf{z}_{\mathbf{w}_{\leftarrow e_{l-1}}} \rho_{\mathbf{w}_{\leftarrow e_{l-1}}}^{-1} \boldsymbol{\nu}_{\leftarrow e_{l-1}}^t + \mathbf{Z}_{\leftarrow e_{l-1}}^t, \mathbf{w}_{\leftarrow e_l} \hat{\boldsymbol{\nu}}_{\leftarrow e_l}^t + \mathbf{Z}_{\leftarrow e_l}^t \right) - \mathbf{w}_{\leftarrow e_l} \rho_{\mathbf{w}_{\leftarrow e_l}}^{-1} \boldsymbol{\nu}_{\leftarrow e_l}^{t+1} \right) \right] \quad (24)$$

$$\hat{\boldsymbol{\nu}}_{\leftarrow e_l}^0, \boldsymbol{\kappa}_{\leftarrow e_l}^{1,1} = \lim_{n \rightarrow \infty} \frac{1}{N} f_{\leftarrow e_l}^0 \left( \mathbf{z}_{\mathbf{w}_{\leftarrow e_l}}, \mathbf{x}_{\leftarrow e_l}^0, \mathbf{x}_{\leftarrow e_{l+1}}^0 \right)^\top f_{\leftarrow e_l}^0 \left( \mathbf{z}_{\mathbf{w}_{\leftarrow e_l}}, \mathbf{x}_{\leftarrow e_l}^0, \mathbf{x}_{\leftarrow e_{l+1}}^0 \right) \quad (25)$$

$$\hat{\boldsymbol{\nu}}_{\leftarrow e_l}^{t+1} = \lim_{N \rightarrow \infty} \frac{1}{N} \mathbb{E} \left[ \sum_{i=1}^N \frac{\partial f_{\leftarrow e_l,i}^t}{\partial \mathbf{z}_{\mathbf{w}_{\leftarrow e_l},i}, \phi_{\leftarrow e_l}} \left( \mathbf{z}_{\mathbf{w}_{\leftarrow e_l}}, \mathbf{z}_{\mathbf{w}_{\leftarrow e_l}} \rho_{\mathbf{w}_{\leftarrow e_l}}^{-1} \boldsymbol{\nu}_{\leftarrow e_l}^t + \mathbf{Z}_{\leftarrow e_l}^t, \mathbf{w}_{\leftarrow e_{l+1}} \hat{\boldsymbol{\nu}}_{\leftarrow e_{l+1}}^t \mathbf{Z}_{\leftarrow e_{l+1}}^t \right) \right] \quad (26)$$

$$\boldsymbol{\kappa}_{\leftarrow e_l}^{s+1,t+1} = \lim_{n \rightarrow \infty} \frac{1}{N} \mathbb{E} \left[ f_{\leftarrow e_l}^s \left( \mathbf{z}_{\mathbf{w}_{\leftarrow e_l}}, \mathbf{z}_{\mathbf{w}_{\leftarrow e_l}} \rho_{\mathbf{w}_{\leftarrow e_l}}^{-1} \boldsymbol{\nu}_{\leftarrow e_l}^s + \mathbf{Z}_{\leftarrow e_l}^s, \mathbf{w}_{\leftarrow e_{l+1}} \hat{\boldsymbol{\nu}}_{\leftarrow e_{l+1}}^s \mathbf{Z}_{\leftarrow e_{l+1}}^s \right)^\top \right. \\ \left. f_{\leftarrow e_l}^t \left( \mathbf{z}_{\mathbf{w}_{\leftarrow e_l}}, \mathbf{z}_{\mathbf{w}_{\leftarrow e_l}} \rho_{\mathbf{w}_{\leftarrow e_l}}^{-1} \boldsymbol{\nu}_{\leftarrow e_l}^t + \mathbf{Z}_{\leftarrow e_l}^t, \mathbf{w}_{\leftarrow e_{l+1}} \hat{\boldsymbol{\nu}}_{\leftarrow e_{l+1}}^t \mathbf{Z}_{\leftarrow e_{l+1}}^t \right) \right] \quad (27)$$

- for  $l=L$

$$\boldsymbol{\nu}_{\leftarrow e_L}^0 = \lim_{N \rightarrow \infty} \frac{1}{N} \mathbf{w}_{\leftarrow e_L}^\top f_{\leftarrow e_L}^0(\mathbf{x}_{\leftarrow e_L}^0), \boldsymbol{\kappa}_{\leftarrow e_L}^{1,1} = \lim_{N \rightarrow \infty} \frac{1}{N} f_{\leftarrow e_L}^0(\mathbf{x}_{\leftarrow e_L}^0)^\top f_{\leftarrow e_L}^0(\mathbf{x}_{\leftarrow e_L}^0) \quad (28)$$

$$\boldsymbol{\nu}_{\leftarrow e_L}^{t+1} = \lim_{N \rightarrow +\infty} \frac{1}{N} \mathbb{E} \left[ \mathbf{w}_{\leftarrow e_L}^\top f_{\leftarrow e_L}^t \left( \mathbf{z}_{\mathbf{w}_{\leftarrow e_{L-1}}} \rho_{\mathbf{w}_{\leftarrow e_{L-1}}}^{-1} \boldsymbol{\nu}_{\leftarrow e_{L-1}}^t + \mathbf{Z}_{\leftarrow e_{L-1}}^t, \mathbf{w}_{\leftarrow e_L} \hat{\boldsymbol{\nu}}_{\leftarrow e_L}^t + \mathbf{Z}_{\leftarrow e_L}^t \right) \right] \quad (29)$$

$$\boldsymbol{\kappa}_{\leftarrow e_L}^{s+1,t+1} = \boldsymbol{\kappa}_{\leftarrow e_L}^{t+1,s+1} = \lim_{N \rightarrow +\infty} \quad (30)$$

$$\frac{1}{N} \mathbb{E} \left[ \left( f_{\leftarrow e_L}^s \left( \mathbf{z}_{\mathbf{w}_{\leftarrow e_{L-1}}} \rho_{\mathbf{w}_{\leftarrow e_{L-1}}}^{-1} \boldsymbol{\nu}_{\leftarrow e_{L-1}}^s + \mathbf{Z}_{\leftarrow e_{L-1}}^s, \mathbf{w}_{\leftarrow e_L} \hat{\boldsymbol{\nu}}_{\leftarrow e_L}^s + \mathbf{Z}_{\leftarrow e_L}^s \right) - \mathbf{w}_{\leftarrow e_L} \rho_{\mathbf{w}_{\leftarrow e_L}}^{-1} \boldsymbol{\nu}_{\leftarrow e_L}^{s+1} \right)^\top \right. \right. \\ \left. \left. \left( f_{\leftarrow e_L}^t \left( \mathbf{z}_{\mathbf{w}_{\leftarrow e_{L-1}}} \rho_{\mathbf{w}_{\leftarrow e_{L-1}}}^{-1} \boldsymbol{\nu}_{\leftarrow e_{L-1}}^t + \mathbf{Z}_{\leftarrow e_{L-1}}^t, \mathbf{w}_{\leftarrow e_L} \hat{\boldsymbol{\nu}}_{\leftarrow e_L}^t + \mathbf{Z}_{\leftarrow e_L}^t \right) - \mathbf{w}_{\leftarrow e_L} \rho_{\mathbf{w}_{\leftarrow e_L}}^{-1} \boldsymbol{\nu}_{\leftarrow e_L}^{t+1} \right) \right] \quad (31)$$

$$\hat{\boldsymbol{\nu}}_{\leftarrow e_L}^0, \boldsymbol{\kappa}_{\leftarrow e_L}^{1,1} = \lim_{n \rightarrow \infty} \frac{1}{N} f_{\leftarrow e_L}^0 \left( \mathbf{z}_{\mathbf{w}_{\leftarrow e_L}}, \mathbf{x}_{\leftarrow e_L}^0 \right)^\top f_{\leftarrow e_L}^0 \left( \mathbf{z}_{\mathbf{w}_{\leftarrow e_L}} \right) \quad (32)$$

$$\hat{\boldsymbol{\nu}}_{\leftarrow e_L}^{t+1} = \lim_{N \rightarrow \infty} \frac{1}{N} \mathbb{E} \left[ \sum_{i=1}^N \frac{\partial f_{\leftarrow e_L,i}^t}{\partial \mathbf{z}_{\mathbf{w}_{\leftarrow e_L},i}, \phi_{\leftarrow e_L}} \left( \mathbf{z}_{\mathbf{w}_{\leftarrow e_L}}, \mathbf{z}_{\mathbf{w}_{\leftarrow e_L}} \rho_{\mathbf{w}_{\leftarrow e_L}}^{-1} \boldsymbol{\nu}_{\leftarrow e_L}^t + \mathbf{Z}_{\leftarrow e_L}^t \right) \right] \quad (33)$$

$$\boldsymbol{\kappa}_{\leftarrow e_L}^{s+1,t+1} = \lim_{n \rightarrow \infty} \frac{1}{N} \mathbb{E} \left[ f_{\leftarrow e_L}^s \left( \mathbf{z}_{\mathbf{w}_{\leftarrow e_L}}, \mathbf{z}_{\mathbf{w}_{\leftarrow e_L}} \rho_{\mathbf{w}_{\leftarrow e_L}}^{-1} \boldsymbol{\nu}_{\leftarrow e_L}^s + \mathbf{Z}_{\leftarrow e_L}^s \right)^\top \right. \\ \left. f_{\leftarrow e_L}^t \left( \mathbf{z}_{\mathbf{w}_{\leftarrow e_L}}, \mathbf{z}_{\mathbf{w}_{\leftarrow e_L}} \rho_{\mathbf{w}_{\leftarrow e_L}}^{-1} \boldsymbol{\nu}_{\leftarrow e_L}^t + \mathbf{Z}_{\leftarrow e_L}^t \right) \right] \quad (34)$$

where, for any  $1 \leq l \leq L$ , the symbol  $\partial \mathbf{z}_{\mathbf{w}_{\leftarrow e_l},i}, \phi_{\leftarrow e_l}$  denotes the partial derivative w.r.t. the argument of  $\phi_{\leftarrow e_l}$ ,  $(\mathbf{Z}_{\leftarrow e_l}^1, \dots, \mathbf{Z}_{\leftarrow e_l}^t)$  is a centered Gaussian random vector with covariance  $(\boldsymbol{\kappa}_{\leftarrow e_l}^{r,s})_{r,s \leq t} \otimes \mathbf{I}_{n_w}$  (and similarly for left-oriented edges), and  $\mathbf{z}_{\mathbf{w}_{\leftarrow e_l}}$  is distributed according to  $\mathbf{N}(0, \rho_{\mathbf{w}_{\leftarrow e_l}})$ .

**Theorem A.2.** Assume (A1)-(A7). Define, as above, independently for each  $\leftarrow e_l$ ,  $\mathbf{Z}_{\leftarrow e_l}^0 = \mathbf{x}_{\leftarrow e_l}^0$  and  $(\mathbf{Z}_{\leftarrow e_l}^1, \dots, \mathbf{Z}_{\leftarrow e_l}^t)$  a centered Gaussian random vector of covariance  $(\boldsymbol{\kappa}_{\leftarrow e_l}^{r,s})_{r,s \leq t} \otimes \mathbf{I}_{n_{l-1}}$ . Then for any

sequence of uniformly (in  $n$ ) pseudo-Lipschitz function  $\Phi : (\mathbb{R}^{n_{l-1} \times (t+1)q})^2 \rightarrow \mathbb{R}$ , for any  $1 \leq l \leq L$

$$\Phi \left( \left( \mathbf{x}_{\vec{e}_l}^s \right)_{0 \leq s \leq t}, \left( \mathbf{x}_{\overleftarrow{e}_{l-1}}^s \right)_{0 \leq s \leq t} \right) \stackrel{P}{\simeq} \mathbb{E} \left[ \Phi \left( \left( \mathbf{z}_{\mathbf{w}_{\vec{e}_l}} \rho_{\mathbf{w}_{\vec{e}_l}}^{-1} \boldsymbol{\nu}_{\vec{e}_l}^s + \mathbf{Z}_{\vec{e}_{l-1}}^s \right)_{0 \leq s \leq t}, \left( \mathbf{w}_{\overleftarrow{e}_{l-1}} \hat{\boldsymbol{\nu}}_{\overleftarrow{e}_{l-1}}^s + \mathbf{Z}_{\overleftarrow{e}_{l-1}}^s \right)_{0 \leq s \leq t} \right) \right]$$

In summary, at each time step, the variables associated with right oriented edges  $\mathbf{x}_{\vec{e}_l}$  asymptotically behave as the sum of the ground truth  $\mathbf{w}_{\vec{e}_l}$  reweighted by a  $q \times q$  matrix coefficient  $\hat{\boldsymbol{\nu}}_{\vec{e}_l}$  and a  $n_{l-1} \times q$  random matrix with i.i.d. lines  $\mathbf{Z}_{\vec{e}_l}$  with  $q \times q$  covariance  $\boldsymbol{\kappa}_{\vec{e}_l}$  determined by the function associated to the corresponding left-oriented arrow  $f_{\vec{e}_l}^t$ . Similarly, the variables associated with left oriented edges  $\mathbf{x}_{\overleftarrow{e}_l}$  asymptotically behave as the sum of the linear response to the ground truth  $\mathbf{z}_{\mathbf{w}_{\overleftarrow{e}_l}}$  (asymptotic equivalent of  $\mathbf{A}_{\overleftarrow{e}_l} \mathbf{w}_{\overleftarrow{e}_l}$ ) reweighted by a  $q \times q$  matrix coefficient  $\boldsymbol{\nu}_{\overleftarrow{e}_l}$  and a  $n_l \times q$  random matrix with i.i.d. lines  $\mathbf{Z}_{\overleftarrow{e}_l}$  with  $q \times q$  covariance  $\boldsymbol{\kappa}_{\overleftarrow{e}_l}$  determined by the function associated to the corresponding right-oriented arrow  $f_{\overleftarrow{e}_l}^t$ .

*Proof.* This result is a special case of Lemma 2 from [Gerbelot and Berthier, 2021], with a perturbation where only the left-oriented edges involve an additional dependence on  $\mathbf{A}_{\overleftarrow{e}} \mathbf{w}_{\overleftarrow{e}}$ . The required conditions are the same as in [Gerbelot and Berthier, 2021], barring the subgaussian assumption (A3) which ensures the scaled norm of the  $\mathbf{x}_{\vec{e}}^0, \mathbf{w}_{\overleftarrow{e}}$  are finite with high-probability as  $n \rightarrow \infty$ .  $\square$

### A.3 State evolution for multilayer AMP iterations with random convolutional matrices

The following lemma proves the state evolution equations for a multilayer AMP iteration where the dense Gaussian matrices are replaced with random convolutional ones (MCC from Def.3.2) with variance  $\frac{1}{N}$ , with a vector valued variables, i.e.  $q=1$ , and separable non-linearities. We choose the variance as  $\frac{1}{N}$  to follow the notations of [Gerbelot and Berthier, 2021] for more convenience, recovering the variances of iteration Eq.(4) is a straightforward rescaling as done in [Berthier et al., 2020] and will be discussed in the next section. Assume  $q = 1$  and that, for any  $t \in \mathbb{N}$  and  $1 \leq l \leq L$ , the functions  $f_{\vec{e}_l}^t, f_{\overleftarrow{e}_l}^t$  are separable in all their arguments, i.e there exists scalar valued, pseudo-Lipschitz functions  $\sigma_{\vec{e}_l}^t : \mathbb{R}^2 \rightarrow \mathbb{R}, \sigma_{\overleftarrow{e}_l}^t : \mathbb{R}^3 \rightarrow \mathbb{R}$  (where  $\sigma_{\vec{e}_1}^t : \mathbb{R} \rightarrow \mathbb{R}, \sigma_{\overleftarrow{e}_L}^t : \mathbb{R}^2 \rightarrow \mathbb{R}$ ) such that:

for  $l = 1$ , for any  $1 \leq i \leq n_0$  :

$$f_{\vec{e}_1}^t(\mathbf{x}_{\vec{e}_1}^t)_i = \sigma_{\vec{e}_1}^t(x_{\vec{e}_1,i}^t)$$

for any  $1 \leq l \leq L - 1$ , for any  $1 \leq i \leq n_l$ :

$$f_{\vec{e}_l}^t(\mathbf{A}_{\vec{e}_l} \mathbf{w}_{\vec{e}_l}, \mathbf{x}_{\vec{e}_l}^t, \mathbf{x}_{\overleftarrow{e}_{l+1}}^t)_i = \sigma_{\vec{e}_l}^t((\mathbf{A}_{\vec{e}_l} \mathbf{w}_{\vec{e}_l})_i, x_{\vec{e}_l,i}^t, x_{\overleftarrow{e}_{l+1},i}^t)$$

for any  $2 \leq l \leq L, 1 \leq i \leq n_{l-1}$ :

$$f_{\overleftarrow{e}_l}^t(\mathbf{x}_{\overleftarrow{e}_{l-1}}^t, \mathbf{x}_{\overleftarrow{e}_l}^t)_i = \sigma_{\overleftarrow{e}_l}^t(x_{\overleftarrow{e}_{l-1},i}^t, x_{\overleftarrow{e}_l,i}^t)$$

for  $l=L$ , any  $1 \leq i \leq n_L$ :

$$f_{\overleftarrow{e}_L}^t(\mathbf{A}_{\overleftarrow{e}_L} \mathbf{w}_{\overleftarrow{e}_L}, \mathbf{x}_{\overleftarrow{e}_L}^t)_i = \sigma_{\overleftarrow{e}_L}^t((\mathbf{A}_{\overleftarrow{e}_L} \mathbf{w}_{\overleftarrow{e}_L})_i, x_{\overleftarrow{e}_L,i}^t)$$

Define the following scalar SE equations

- for  $l = 1$ :

$$\nu_{\vec{e}_1}^0 = \delta_0 \mathbb{E} \left[ w_{\vec{e}_1} \sigma_{\vec{e}_1}^0 (x_{\vec{e}_1}^0) \right], \quad \kappa_{\vec{e}_1}^{1,1} = \delta_0 \mathbb{E} \left[ \sigma_{\vec{e}_1}^0 (x_{\vec{e}_1}^0) \sigma_{\vec{e}_1}^0 (x_{\vec{e}_1}^0) \right] \quad (35)$$

$$\nu_{\vec{e}_1}^{t+1} = \delta_0 \mathbb{E} \left[ w_{\vec{e}_1} \sigma_{\vec{e}_1}^t \left( w_{\vec{e}_1} \hat{\nu}_{\vec{e}_1}^t + Z_{\vec{e}_1}^t \right) \right] \quad (36)$$

$$\begin{aligned} \kappa_{\vec{e}_1}^{s+1,t+1} = \kappa_{\vec{e}_1}^{t+1,s+1} = \delta_0 \mathbb{E} & \left[ \left( \sigma_{\vec{e}_1}^s \left( w_{\vec{e}_1} \hat{\nu}_{\vec{e}_1}^s + Z_{\vec{e}_1}^s \right) - w_{\vec{e}_1} \rho_{w_{\vec{e}_1}}^{-1} \nu_{\vec{e}_1}^{s+1} \right) \right. \\ & \left. \left( \sigma_{\vec{e}_1}^t \left( w_{\vec{e}_1} \hat{\nu}_{\vec{e}_1}^t + Z_{\vec{e}_1}^t \right) - w_{\vec{e}_1} \rho_{w_{\vec{e}_1}}^{-1} \nu_{\vec{e}_1}^{t+1} \right) \right] \quad (37) \end{aligned}$$

$$\hat{\nu}_{\vec{e}_1}^0, \kappa_{\vec{e}_1}^{1,1} = \delta_1 \mathbb{E} \left[ \sigma_{\vec{e}_1}^0 \left( z_{w_{\vec{e}_1}}, x_{\vec{e}_1}^0, x_{\vec{e}_2}^0 \right) \sigma_{\vec{e}_1}^0 \left( z_{w_{\vec{e}_1}}, x_{\vec{e}_1}^0, x_{\vec{e}_2}^0 \right) \right] \quad (38)$$

$$\hat{\nu}_{\vec{e}_1}^{t+1} = \delta_1 \mathbb{E} \left[ \frac{\partial \sigma_{\vec{e}_1}^t}{\partial z_{w_{\vec{e}_1}, i}, \phi_{\vec{e}_1}} \left( z_{w_{\vec{e}_1}}, z_{w_{\vec{e}_1}} \rho_{w_{\vec{e}_1}}^{-1} \nu_{\vec{e}_1}^t + Z_{\vec{e}_1}^t, w_{\vec{e}_2} \hat{\nu}_{\vec{e}_2}^t + Z_{\vec{e}_2}^t \right) \right] \quad (39)$$

$$\begin{aligned} \kappa_{\vec{e}_1}^{s+1,t+1} = \delta_1 \mathbb{E} & \left[ \sigma_{\vec{e}_1}^s \left( z_{w_{\vec{e}_1}}, z_{w_{\vec{e}_1}} \rho_{w_{\vec{e}_1}}^{-1} \nu_{\vec{e}_1}^s + Z_{\vec{e}_1}^s, w_{\vec{e}_2} \hat{\nu}_{\vec{e}_2}^s + Z_{\vec{e}_2}^s \right) \right. \\ & \left. \sigma_{\vec{e}_1}^t \left( z_{w_{\vec{e}_1}}, z_{w_{\vec{e}_1}} \rho_{w_{\vec{e}_1}}^{-1} \nu_{\vec{e}_1}^t + Z_{\vec{e}_1}^t, w_{\vec{e}_2} \hat{\nu}_{\vec{e}_2}^t + Z_{\vec{e}_2}^t \right) \right] \quad (40) \end{aligned}$$

- for any  $2 \leq l \leq L-1$

$$\nu_{\vec{e}_l}^0 = \delta_{n_{l-1}} \mathbb{E} \left[ w_{\vec{e}_l} \sigma_{\vec{e}_l}^0 (x_{\vec{e}_l}^0) \right], \quad \kappa_{\vec{e}_l}^{1,1} = \delta_{n_{l-1}} \mathbb{E} \left[ \sigma_{\vec{e}_l}^0 (x_{\vec{e}_l}^0) \sigma_{\vec{e}_l}^0 (x_{\vec{e}_l}^0) \right] \quad (41)$$

$$\nu_{\vec{e}_l}^{t+1} = \delta_{n_{l-1}} \mathbb{E} \left[ w_{\vec{e}_l} \sigma_{\vec{e}_l}^t \left( z_{w_{\vec{e}_{l-1}}} \rho_{w_{\vec{e}_{l-1}}}^{-1} \nu_{\vec{e}_{l-1}}^t + Z_{\vec{e}_{l-1}}^t, w_{\vec{e}_l} \hat{\nu}_{\vec{e}_l}^t + Z_{\vec{e}_l}^t \right) \right] \quad (42)$$

$$\kappa_{\vec{e}_l}^{s+1,t+1} = \kappa_{\vec{e}_l}^{t+1,s+1} = \quad (43)$$

$$\begin{aligned} \delta_{n_{l-1}} \mathbb{E} & \left[ \left( \sigma_{\vec{e}_l}^s \left( z_{w_{\vec{e}_{l-1}}} \rho_{w_{\vec{e}_{l-1}}}^{-1} \nu_{\vec{e}_{l-1}}^s + Z_{\vec{e}_{l-1}}^s, w_{\vec{e}_l} \hat{\nu}_{\vec{e}_l}^s + Z_{\vec{e}_l}^s \right) - w_{\vec{e}_l} \rho_{w_{\vec{e}_l}}^{-1} \nu_{\vec{e}_l}^{s+1} \right) \right. \\ & \left. \left( \sigma_{\vec{e}_l}^t \left( z_{w_{\vec{e}_{l-1}}} \rho_{w_{\vec{e}_{l-1}}}^{-1} \nu_{\vec{e}_{l-1}}^t + Z_{\vec{e}_{l-1}}^t, w_{\vec{e}_l} \hat{\nu}_{\vec{e}_l}^t + Z_{\vec{e}_l}^t \right) - w_{\vec{e}_l} \rho_{w_{\vec{e}_l}}^{-1} \nu_{\vec{e}_l}^{t+1} \right) \right] \quad (44) \end{aligned}$$

$$\hat{\nu}_{\vec{e}_l}^0, \kappa_{\vec{e}_l}^{1,1} = \delta_{n_l} \mathbb{E} \left[ \sigma_{\vec{e}_l}^0 \left( z_{w_{\vec{e}_l}}, x_{\vec{e}_l}^0, x_{\vec{e}_{l+1}}^0 \right) \sigma_{\vec{e}_l}^0 \left( z_{w_{\vec{e}_l}}, x_{\vec{e}_l}^0, x_{\vec{e}_{l+1}}^0 \right) \right] \quad (45)$$

$$\hat{\nu}_{\vec{e}_l}^{t+1} = \delta_{n_l} \mathbb{E} \left[ \frac{\partial \sigma_{\vec{e}_l}^t}{\partial z_{w_{\vec{e}_l}, i}, \phi_{\vec{e}_l}} \left( z_{w_{\vec{e}_l}}, z_{w_{\vec{e}_l}} \rho_{w_{\vec{e}_l}}^{-1} \nu_{\vec{e}_l}^t + Z_{\vec{e}_l}^t, w_{\vec{e}_{l+1}} \hat{\nu}_{\vec{e}_{l+1}}^t + Z_{\vec{e}_{l+1}}^t \right) \right] \quad (46)$$

$$\begin{aligned} \kappa_{\vec{e}_l}^{s+1,t+1} = \delta_{n_l} \mathbb{E} & \left[ \sigma_{\vec{e}_l}^s \left( z_{w_{\vec{e}_l}}, z_{w_{\vec{e}_l}} \rho_{w_{\vec{e}_l}}^{-1} \nu_{\vec{e}_l}^s + Z_{\vec{e}_l}^s, w_{\vec{e}_{l+1}} \hat{\nu}_{\vec{e}_{l+1}}^s + Z_{\vec{e}_{l+1}}^s \right) \right. \\ & \left. \sigma_{\vec{e}_l}^t \left( z_{w_{\vec{e}_l}}, z_{w_{\vec{e}_l}} \rho_{w_{\vec{e}_l}}^{-1} \nu_{\vec{e}_l}^t + Z_{\vec{e}_l}^t, w_{\vec{e}_{l+1}} \hat{\nu}_{\vec{e}_{l+1}}^t + Z_{\vec{e}_{l+1}}^t \right) \right] \quad (47) \end{aligned}$$

- for  $l=L$

$$\nu_{\vec{e}_L}^0 = \delta_{n_{L-1}} \mathbb{E} \left[ w_{\vec{e}_L} \sigma_{\vec{e}_L}^0 (x_{\vec{e}_L}^0) \right], \quad \kappa_{\vec{e}_L}^{1,1} = \delta_{n_{L-1}} \mathbb{E} \left[ \sigma_{\vec{e}_L}^0 (x_{\vec{e}_L}^0) \sigma_{\vec{e}_L}^0 (x_{\vec{e}_L}^0) \right] \quad (48)$$

$$\nu_{\vec{e}_L}^{t+1} = \delta_{n_{L-1}} \mathbb{E} \left[ w_{\vec{e}_L} \sigma_{\vec{e}_L}^t \left( z_{w_{\vec{e}_L}} \rho_{w_{\vec{e}_L}}^{-1} \nu_{\vec{e}_L}^t + Z_{\vec{e}_L}^t, w_{\vec{e}_L} \hat{\nu}_{\vec{e}_L}^t + Z_{\vec{e}_L}^t \right) \right] \quad (49)$$

$$\kappa_{\vec{e}_L}^{s+1,t+1} = \kappa_{\vec{e}_L}^{t+1,s+1} = \quad (50)$$

$$\delta_{n_{L-1}} \mathbb{E} \left[ \left( \sigma_{\vec{e}_L}^s \left( z_{w_{\vec{e}_L}} \rho_{w_{\vec{e}_L}}^{-1} \nu_{\vec{e}_L}^s + Z_{\vec{e}_L}^s, w_{\vec{e}_L} \hat{\nu}_{\vec{e}_L}^s + Z_{\vec{e}_L}^s \right) - w_{\vec{e}_L} \rho_{w_{\vec{e}_L}}^{-1} \nu_{\vec{e}_L}^{s+1} \right) \left( \sigma_{\vec{e}_L}^t \left( z_{w_{\vec{e}_L}} \rho_{w_{\vec{e}_L}}^{-1} \nu_{\vec{e}_L}^t + Z_{\vec{e}_L}^t, w_{\vec{e}_L} \hat{\nu}_{\vec{e}_L}^t + Z_{\vec{e}_L}^t \right) - w_{\vec{e}_L} \rho_{w_{\vec{e}_L}}^{-1} \nu_{\vec{e}_L}^{t+1} \right) \right] \quad (51)$$

$$\hat{\nu}_{\vec{e}_L}^0, \kappa_{\vec{e}_L}^{1,1} = \delta_{n_L} \mathbb{E} \left[ \sigma_{\vec{e}_L}^0 \left( z_{w_{\vec{e}_L}}, x_{\vec{e}_L}^0 \right) \sigma_{\vec{e}_L}^0 \left( z_{w_{\vec{e}_L}} \right) \right] \quad (52)$$

$$\hat{\nu}_{\vec{e}_L}^{t+1} = \delta_{n_L} \mathbb{E} \left[ \frac{\partial \sigma_{\vec{e}_L}^{t,i}}{\partial z_{w_{\vec{e}_L}}, i, \phi_{\vec{e}_L}^t} \left( z_{w_{\vec{e}_L}}, z_{w_{\vec{e}_L}} \rho_{w_{\vec{e}_L}}^{-1} \nu_{\vec{e}_L}^t + Z_{\vec{e}_L}^t \right) \right] \quad (53)$$

$$\kappa_{\vec{e}_L}^{s+1,t+1} = \delta_{n_L} \mathbb{E} \left[ \sigma_{\vec{e}_L}^s \left( z_{w_{\vec{e}_L}}, z_{w_{\vec{e}_L}} \rho_{w_{\vec{e}_L}}^{-1} \nu_{\vec{e}_L}^s + Z_{\vec{e}_L}^s \right) \sigma_{\vec{e}_L}^t \left( z_{w_{\vec{e}_L}}, z_{w_{\vec{e}_L}} \rho_{w_{\vec{e}_L}}^{-1} \nu_{\vec{e}_L}^t + Z_{\vec{e}_L}^t \right) \right] \quad (54)$$

**Lemma A.3.** Under the assumptions of section A.3, define, as above, independently for each  $\vec{e}_l$ ,  $Z_{\vec{e}_l}^0 = x_{\vec{e}_l}^0$  and  $(Z_{\vec{e}_l}^1, \dots, Z_{\vec{e}_l}^t)$  a centered Gaussian random vector of covariance  $(\kappa_{\vec{e}_l}^{r,s})_{r,s \leq t}$  (and similarly for left-oriented edges). Then for any  $1 \leq l \leq L$ , for any sequence of uniformly (in  $n$ ) pseudo-Lipschitz function  $\Phi_l : (\mathbb{R}^{n_{l-1} \times (t+1)})^2 \rightarrow \mathbb{R}$

$$\Phi \left( \left( \mathbf{x}_{\vec{e}_l}^s \right)_{0 \leq s \leq t}, \left( \mathbf{x}_{\vec{e}_l}^s \right)_{0 \leq s \leq t, \vec{e}_{l-1} \in \overleftarrow{E}} \right) \stackrel{P}{\simeq} \mathbb{E} \left[ \Phi \left( \left( z_{w_{\vec{e}_l}} \rho_{w_{\vec{e}_l}}^{-1} \nu_{\vec{e}_l}^s + Z_{\vec{e}_l}^s \right)_{0 \leq s \leq t, \vec{e}_l \in \overleftarrow{E}}, \left( w_{\vec{e}_{l-1}} \hat{\nu}_{\vec{e}_{l-1}}^s + Z_{\vec{e}_{l-1}}^s \right)_{0 \leq s \leq t} \right) \right]$$

*Proof.* Consider the following iteration, corresponding to the algorithm presented in the previous section Eq.(56) with  $q = 1$  indexed on the same graph as above, but where the matrices  $\mathbf{A}_{\vec{e}_l}$  are replaced with random convolutional ones, denoted  $\hat{\mathbf{A}}_{\vec{e}_l}$  such that

$$\forall \vec{e} \in \overrightarrow{E} \quad \hat{\mathbf{A}}_{\vec{e}} \sim \mathcal{M}(D_{\vec{e}}, P_{\vec{e}}, k_{\vec{e}}, q_{\vec{e}}) \quad (55)$$

where  $\mathbf{A}_{\vec{e}_l} \in \mathbb{R}^{D_{\vec{e}_l} q_{\vec{e}_l} \times P_{\vec{e}_l} q_{\vec{e}_l}}$ , and we remind that we chose variances of  $1/N$ . Since we assume that  $q = 1$ , thus the Onsager terms are scalars, which we denote with lowercase letters  $b_{\vec{e}}^t$ . The corresponding

iteration then reads:

$$\begin{aligned}
\mathbf{x}_{e_1}^{t+1} &= \hat{\mathbf{A}}_{e_1} \mathbf{m}_{e_1}^t - b_{e_1}^t \mathbf{m}_{e_1}^{t-1}, \\
\mathbf{m}_{e_1}^t &= f_{e_1}^t(\mathbf{x}_{e_1}^t), \\
\mathbf{x}_{e_1}^{t+1} &= \hat{\mathbf{A}}_{e_1}^\top \mathbf{m}_{e_1}^t - b_{e_1}^t \mathbf{m}_{e_1}^{t-1}, \\
\mathbf{m}_{e_1}^t &= f_{e_1}^t(\hat{\mathbf{A}}_{e_1} \mathbf{w}_{e_1}, \mathbf{x}_{e_1}^t, \mathbf{x}_{e_2}^t), \\
\\
\mathbf{x}_{e_2}^{t+1} &= \hat{\mathbf{A}}_{e_2} \mathbf{m}_{e_2}^t - b_{e_2}^t \mathbf{m}_{e_2}^{t-1}, \\
\mathbf{m}_{e_2}^t &= f_{e_2}^t(\mathbf{x}_{e_1}^t, \mathbf{x}_{e_2}^t), \\
\mathbf{x}_{e_2}^{t+1} &= \hat{\mathbf{A}}_{e_2}^\top \mathbf{m}_{e_2}^t - b_{e_2}^t \mathbf{m}_{e_2}^{t-1}, \\
\mathbf{m}_{e_2}^t &= f_{e_2}^t(\hat{\mathbf{A}}_{e_2} \mathbf{w}_{e_2}, \mathbf{x}_{e_2}^t, \mathbf{x}_{e_3}^t), \\
\\
&\vdots \\
\\
\mathbf{x}_{e_L}^{t+1} &= \hat{\mathbf{A}}_{e_L} \mathbf{m}_{e_L}^t - b_{e_L}^t \mathbf{m}_{e_L}^{t-1}, \\
\mathbf{m}_{e_L}^t &= f_{e_L}^t(\mathbf{x}_{e_{L-1}}^t, \mathbf{x}_{e_L}^t), \\
\mathbf{x}_{e_L}^{t+1} &= \hat{\mathbf{A}}_{e_L}^\top \mathbf{m}_{e_L}^t - b_{e_L}^t \mathbf{m}_{e_L}^{t-1}, \\
\mathbf{m}_{e_L}^t &= f_{e_L}^t(\hat{\mathbf{A}}_{e_L} \mathbf{w}_{e_L}, \mathbf{x}_{e_L}^t)
\end{aligned} \tag{56}$$

Then, according to Lemma 4.3, for any  $1 \leq l \leq L$ , there exists a pair of orthogonal matrices  $\mathbf{U}_{e_l} \in \mathbb{R}^{D_{e_l} q_{e_l} \times D_{e_l} q_{e_l}}$ ,  $\mathbf{V}_{e_l} \in \mathbb{R}^{P_{e_l} q_{e_l} \times P_{e_l} q_{e_l}}$  such that  $\hat{\mathbf{A}}_{e_l} = \mathbf{U}_{e_l} \tilde{\mathbf{A}}_{e_l} \mathbf{V}_{e_l}^\top$  and  $\tilde{\mathbf{A}}_{e_l} = \left[ \left( \mathcal{P}_{P_{e_l}, q_{e_l}} \right)^{i-1} \mathbf{Q}_{e_l} \right]_{i=1}^{q_{e_l}}$ , where  $\mathbf{Q}_{e_l} \in \mathbb{R}^{D_{e_l} \times P_{e_l} q_{e_l}}$  is composed of  $q_{e_l}$  blocks of size  $D_{e_l} \times P_{e_l}$ , denoted  $\mathbf{Q}_{e_l}^j$ , verifying

- for any  $1 \leq j \leq k_{e_l}$ ,  $\mathbf{Q}_{e_l}^j$  has i.i.d.  $\mathcal{N}(0, \frac{1}{N})$  elements
- for any  $k_{e_l} < j \leq q_{e_l}$ , all elements of  $\mathbf{Q}_{e_l}^j$  are zero.

In the preceding definition of  $\tilde{\mathbf{A}}_{e_l}$ ,  $\mathbf{Q}_{e_l}$  is understood as a vector of size  $\mathbb{R}^{P_{e_l} q_{e_l}}$  with elements in  $\mathbb{R}^{D_{e_l}}$ , such that the permutation matrix  $\mathcal{P}_{P_{e_l}, q_{e_l}}$  shifts blocks of size  $D_{e_l} \times P_{e_l}$ , yielding

$$\tilde{\mathbf{A}}_{e_l} = \begin{bmatrix} \mathbf{Q}_{e_l}^{(1)} & \mathbf{Q}_{e_l}^{(2)} & \dots & \mathbf{Q}_{e_l}^{(k_{e_l})} & & & \\ & \mathbf{Q}_{e_l}^{(1)} & \mathbf{Q}_{e_l}^{(2)} & \dots & \mathbf{Q}_{e_l}^{(k_{e_l})} & & \\ & & \mathbf{Q}_{e_l}^{(1)} & \mathbf{Q}_{e_l}^{(2)} & \dots & \mathbf{Q}_{e_l}^{(k_{e_l})} & \vdots \\ \vdots & \vdots & \ddots & & & & \\ \mathbf{Q}_{e_l}^{(2)} & \mathbf{Q}_{e_l}^{(3)} & \dots & \mathbf{Q}_{e_l}^{(k_{e_l})} & & & \mathbf{Q}_{e_l}^{(1)} \end{bmatrix} \tag{57}$$

The iteration then reads

$$\begin{aligned}
\mathbf{x}_{e_1}^{t+1} &= \mathbf{U}_{\rightarrow e_1} \tilde{\mathbf{A}}_{\rightarrow e_1} \mathbf{V}_{\rightarrow e_1}^\top \mathbf{m}_{e_1}^t - b_{e_1}^t \mathbf{m}_{e_1}^{t-1}, \\
\mathbf{m}_{e_1}^t &= f_{\rightarrow e_1}^t \left( \mathbf{x}_{e_1}^t \right), \\
\mathbf{x}_{e_1}^{t+1} &= \mathbf{V}_{\rightarrow e_1} \tilde{\mathbf{A}}_{\rightarrow e_1}^\top \mathbf{U}_{\rightarrow e_1}^\top \mathbf{m}_{e_1}^t - b_{e_1}^t \mathbf{m}_{e_1}^{t-1}, \\
\mathbf{m}_{e_1}^t &= f_{e_1}^t \left( \mathbf{U}_{\rightarrow e_1} \tilde{\mathbf{A}}_{\rightarrow e_1} \mathbf{V}_{\rightarrow e_1}^\top \mathbf{w}_{\rightarrow e_1}, \mathbf{x}_{e_1}^t, \mathbf{x}_{e_2}^t \right), \\
\\
\mathbf{x}_{e_2}^{t+1} &= \mathbf{U}_{\rightarrow e_2} \tilde{\mathbf{A}}_{\rightarrow e_2} \mathbf{V}_{\rightarrow e_2}^\top \mathbf{m}_{e_2}^t - b_{e_2}^t \mathbf{m}_{e_2}^{t-1}, \\
\mathbf{m}_{e_2}^t &= f_{\rightarrow e_2}^t \left( \mathbf{x}_{e_1}^t, \mathbf{x}_{e_2}^t \right), \\
\mathbf{x}_{e_2}^{t+1} &= \mathbf{V}_{\rightarrow e_2} \tilde{\mathbf{A}}_{\rightarrow e_2}^\top \mathbf{U}_{\rightarrow e_2}^\top \mathbf{m}_{e_2}^t - b_{e_2}^t \mathbf{m}_{e_2}^{t-1}, \\
\mathbf{m}_{e_2}^t &= f_{e_2}^t \left( \mathbf{U}_{\rightarrow e_2} \tilde{\mathbf{A}}_{\rightarrow e_2} \mathbf{V}_{\rightarrow e_2}^\top \mathbf{w}_{\rightarrow e_2}, \mathbf{x}_{e_2}^t, \mathbf{x}_{e_3}^t \right), \\
\\
&\vdots \\
\\
\mathbf{x}_{e_L}^{t+1} &= \mathbf{U}_{\rightarrow e_L} \tilde{\mathbf{A}}_{\rightarrow e_L} \mathbf{V}_{\rightarrow e_L}^\top \mathbf{m}_{e_L}^t - b_{e_L}^t \mathbf{m}_{e_L}^{t-1}, \\
\mathbf{m}_{e_L}^t &= f_{\rightarrow e_L}^t \left( \mathbf{x}_{\rightarrow e_{L-1}}^t, \mathbf{x}_{e_L}^t \right), \\
\mathbf{x}_{e_L}^{t+1} &= \mathbf{V}_{\rightarrow e_L} \tilde{\mathbf{A}}_{\rightarrow e_L}^\top \mathbf{U}_{\rightarrow e_L}^\top \mathbf{m}_{e_L}^t - b_{e_L}^t \mathbf{m}_{e_L}^{t-1}, \\
\mathbf{m}_{e_L}^t &= f_{e_L}^t \left( \mathbf{U}_{\rightarrow e_L} \tilde{\mathbf{A}}_{\rightarrow e_L} \mathbf{V}_{\rightarrow e_L}^\top \mathbf{w}_{\rightarrow e_L}, \mathbf{x}_{e_L}^t \right)
\end{aligned} \tag{58}$$

Since we will not be making any change of variable on the  $\mathbf{w}_{\rightarrow e_l}$ , we will keep the  $\hat{\mathbf{A}}_{\rightarrow e_l}$  notation for the quantities related to the planted model. Define, for any  $1 \leq l \leq L$  and any  $t \in \mathbb{N}$ :

$$\begin{aligned}
\tilde{\mathbf{x}}_{\rightarrow e_l} &= \mathbf{U}_{\rightarrow e_l}^\top \mathbf{x}_{\rightarrow e_l} & \tilde{\mathbf{x}}_{e_l} &= \mathbf{V}_{\rightarrow e_l}^\top \mathbf{x}_{e_l} \\
\tilde{\mathbf{m}}_{\rightarrow e_l}^t &= \mathbf{V}_{\rightarrow e_l}^\top \mathbf{m}_{\rightarrow e_l}^t & \tilde{\mathbf{m}}_{e_l}^t &= \mathbf{U}_{\rightarrow e_l}^\top \mathbf{m}_{e_l}^t \\
\tilde{f}_{\rightarrow e_1}^t(\tilde{\mathbf{x}}_{e_1}^t) &= \mathbf{V}_{\rightarrow e_1}^\top f_{\rightarrow e_1}^t \left( \mathbf{V}_{\rightarrow e_1} \tilde{\mathbf{x}}_{e_1}^t \right) \\
\tilde{f}_{e_1}^t \left( \hat{\mathbf{A}}_{\rightarrow e_1} \mathbf{w}_{\rightarrow e_1}, \tilde{\mathbf{x}}_{e_1}^t, \tilde{\mathbf{x}}_{e_2}^t \right) &= \mathbf{U}_{\rightarrow e_1}^\top f_{e_1}^t \left( \hat{\mathbf{A}}_{\rightarrow e_1} \mathbf{w}_{\rightarrow e_1}, \mathbf{U}_{\rightarrow e_1} \tilde{\mathbf{x}}_{e_1}^t, \mathbf{V}_{\rightarrow e_2} \tilde{\mathbf{x}}_{e_2}^t \right) \\
\tilde{f}_{\rightarrow e_2}^t \left( \tilde{\mathbf{x}}_{e_1}^t, \tilde{\mathbf{x}}_{e_2}^t \right) &= \mathbf{V}_{\rightarrow e_2}^\top f_{\rightarrow e_2}^t \left( \mathbf{U}_{\rightarrow e_1} \tilde{\mathbf{x}}_{e_1}^t, \mathbf{V}_{\rightarrow e_2} \tilde{\mathbf{x}}_{e_2}^t \right) \\
\tilde{f}_{e_2}^t \left( \hat{\mathbf{A}}_{\rightarrow e_2} \mathbf{w}_{\rightarrow e_2}, \tilde{\mathbf{x}}_{e_2}^t, \tilde{\mathbf{x}}_{e_3}^t \right) &= \mathbf{U}_{\rightarrow e_2}^\top f_{e_2}^t \left( \hat{\mathbf{A}}_{\rightarrow e_2} \mathbf{w}_{\rightarrow e_2}, \mathbf{U}_{\rightarrow e_2} \tilde{\mathbf{x}}_{e_2}^t, \mathbf{V}_{\rightarrow e_3} \tilde{\mathbf{x}}_{e_3}^t \right) \\
&\vdots \\
\tilde{f}_{\rightarrow e_L}^t \left( \tilde{\mathbf{x}}_{\rightarrow e_{L-1}}^t, \tilde{\mathbf{x}}_{e_L}^t \right) &= \mathbf{V}_{\rightarrow e_L}^\top f_{\rightarrow e_L}^t \left( \mathbf{U}_{\rightarrow e_{L-1}} \tilde{\mathbf{x}}_{\rightarrow e_{L-1}}^t, \mathbf{V}_{\rightarrow e_L} \tilde{\mathbf{x}}_{e_L}^t \right) \\
\tilde{f}_{e_L}^t \left( \hat{\mathbf{A}}_{\rightarrow e_L} \mathbf{w}_{\rightarrow e_L}, \tilde{\mathbf{x}}_{e_L}^t \right) &= \mathbf{U}_{\rightarrow e_L}^\top f_{e_L}^t \left( \mathbf{U}_{\rightarrow e_L} \tilde{\mathbf{A}}_{\rightarrow e_L} \mathbf{V}_{\rightarrow e_L} \mathbf{w}_{\rightarrow e_L}, \mathbf{U}_{\rightarrow e_L} \tilde{\mathbf{x}}_{e_L}^t \right)
\end{aligned}$$

Using the orthogonality of the permutation matrices  $\mathbf{U}_{\vec{e}}$ ,  $\mathbf{V}_{\vec{e}}$ , the iteration may be rewritten

$$\begin{aligned}
\tilde{\mathbf{x}}_{e_1}^{t+1} &= \tilde{\mathbf{A}}_{\vec{e}_1} \tilde{\mathbf{m}}_{e_1}^t - b_{e_1}^t \tilde{\mathbf{m}}_{e_1}^{t-1}, \\
\tilde{\mathbf{m}}_{e_1}^t &= \tilde{f}_{\vec{e}_1}^t(\tilde{\mathbf{x}}_{e_1}^t), \\
\tilde{\mathbf{x}}_{e_1}^{t+1} &= \tilde{\mathbf{A}}_{\vec{e}_1}^\top \tilde{\mathbf{m}}_{e_1}^t - b_{e_1}^t \tilde{\mathbf{m}}_{e_1}^{t-1}, \\
\tilde{\mathbf{m}}_{e_1}^t &= \tilde{f}_{e_1}^t \left( \hat{\mathbf{A}}_{\vec{e}_1} \mathbf{w}_{\vec{e}_1}, \tilde{\mathbf{x}}_{e_1}^t, \tilde{\mathbf{x}}_{e_2}^t \right), \\
\\
\tilde{\mathbf{x}}_{e_2}^{t+1} &= \tilde{\mathbf{A}}_{\vec{e}_2} \tilde{\mathbf{m}}_{e_2}^t - b_{e_2}^t \tilde{\mathbf{m}}_{e_2}^{t-1}, \\
\tilde{\mathbf{m}}_{e_2}^t &= \tilde{f}_{\vec{e}_2}^t \left( \tilde{\mathbf{x}}_{e_1}^t, \tilde{\mathbf{x}}_{e_2}^t \right), \\
\tilde{\mathbf{x}}_{e_2}^{t+1} &= \tilde{\mathbf{A}}_{\vec{e}_2}^\top \tilde{\mathbf{m}}_{e_2}^t - b_{e_2}^t \tilde{\mathbf{m}}_{e_2}^{t-1}, \\
\tilde{\mathbf{m}}_{e_2}^t &= \tilde{f}_{e_2}^t \left( \hat{\mathbf{A}}_{\vec{e}_2} \mathbf{w}_{\vec{e}_2}, \tilde{\mathbf{x}}_{e_2}^t, \tilde{\mathbf{x}}_{e_3}^t \right), \\
\\
&\vdots \\
\\
\tilde{\mathbf{x}}_{e_L}^{t+1} &= \tilde{\mathbf{A}}_{\vec{e}_L} \tilde{\mathbf{m}}_{e_L}^t - b_{e_L}^t \tilde{\mathbf{m}}_{e_L}^{t-1}, \\
\tilde{\mathbf{m}}_{e_L}^t &= \tilde{f}_{\vec{e}_L}^t \left( \tilde{\mathbf{x}}_{e_{L-1}}^t, \tilde{\mathbf{x}}_{e_L}^t \right), \\
\tilde{\mathbf{x}}_{e_L}^{t+1} &= \tilde{\mathbf{A}}_{\vec{e}_L}^\top \tilde{\mathbf{m}}_{e_L}^t - b_{e_L}^t \tilde{\mathbf{m}}_{e_L}^{t-1}, \\
\tilde{\mathbf{m}}_{e_L}^t &= \tilde{f}_{e_L}^t \left( \hat{\mathbf{A}}_{\vec{e}_L} \mathbf{w}_{\vec{e}_L}, \tilde{\mathbf{x}}_{e_L}^t \right)
\end{aligned} \tag{59}$$

Recall, for any  $1 \leq l \leq L$ , the dimensions  $\tilde{\mathbf{A}}_{\vec{e}_l} \in \mathbb{R}^{D_{\vec{e}_l} q_{\vec{e}_l} \times P_{\vec{e}_l} q_{\vec{e}_l}}$  and  $\tilde{f}_{\vec{e}_l}^t(\dots) \in \mathbb{R}^{P_{\vec{e}_l} q_{\vec{e}_l}}$ . Consider then

$$\tilde{f}_{\vec{e}_l}^t(\dots) = \begin{bmatrix} \left( \tilde{f}_{\vec{e}_l}^t \right)^{(1)}(\dots) \\ \vdots \\ \left( \tilde{f}_{\vec{e}_l}^t \right)^{(q_{\vec{e}_l})}(\dots) \end{bmatrix} \tag{60}$$

where, for any  $1 \leq k \leq q_{\vec{e}_l}$ ,  $\left( \tilde{f}_{\vec{e}_l}^t \right)^{(k)}(\dots) \in \mathbb{R}^{P_{\vec{e}_l}}$ . The product  $\tilde{\mathbf{A}}_{\vec{e}_l} \tilde{f}_{\vec{e}_l}^t(\dots) \in \mathbb{R}^{D_{\vec{e}_l} q_{\vec{e}_l}}$  then reads, using the circulant structure of  $\tilde{\mathbf{A}}_{\vec{e}_l}$

$$\begin{bmatrix} \mathbf{Q}_{\vec{e}_l}^{(1)} & \mathbf{Q}_{\vec{e}_l}^{(2)} & \dots & \mathbf{Q}_{\vec{e}_l}^{(k_{\vec{e}_l})} \\ & \mathbf{Q}_{\vec{e}_l}^{(1)} & \mathbf{Q}_{\vec{e}_l}^{(2)} & \dots & \mathbf{Q}_{\vec{e}_l}^{(k_{\vec{e}_l})} \\ & & \mathbf{Q}_{\vec{e}_l}^{(1)} & \mathbf{Q}_{\vec{e}_l}^{(2)} & \dots & \mathbf{Q}_{\vec{e}_l}^{(k_{\vec{e}_l})} \\ \vdots & \vdots & \ddots & & & \vdots \\ \mathbf{Q}_{\vec{e}_l}^{(2)} & \mathbf{Q}_{\vec{e}_l}^{(3)} & \dots & \mathbf{Q}_{\vec{e}_l}^{(k_{\vec{e}_l})} & & \mathbf{Q}_{\vec{e}_l}^{(1)} \end{bmatrix} \begin{bmatrix} \left( \tilde{f}_{\vec{e}_l}^t \right)^{(1)}(\dots) \\ \vdots \\ \left( \tilde{f}_{\vec{e}_l}^t \right)^{(q_{\vec{e}_l})}(\dots) \end{bmatrix} \tag{61}$$

$$= \left[ \left( \left( \mathcal{P}_{P_{\vec{e}_l}, q_{\vec{e}_l}} \right)^{i-1} \mathbf{Q}_{\vec{e}_l} \right) \tilde{f}_{\vec{e}_l}^t(\dots) \right]_{i=1}^{q_{\vec{e}_l}} \tag{62}$$

$$= \left[ \sum_{j=1}^{k_{\vec{e}_l}} \mathbf{Q}_{\vec{e}_l}^{(j)} \left( \tilde{f}_{\vec{e}_l}^t \right)^{(\lfloor j+n-2 \rfloor_{q_{\vec{e}_l}} + 1)}(\dots) \right]_{n=1}^{q_{\vec{e}_l}} \tag{63}$$



where the notation  $[\cdot]_{q_{\vec{e}_l}}$  denotes the modulo  $q_{\vec{e}_l}$ , i.e. the remainder of the euclidian division by  $q_{\vec{e}_l}$ . Now define

$$\tilde{F}_{\vec{e}_l}^t(\dots) = \begin{bmatrix} \left[ \left( \mathcal{P}_{P_{\vec{e}_l}, q_{\vec{e}_l}} \right)^{1-i} \left[ (\tilde{f}_{\vec{e}_l}^t)^{(1)} \dots (\tilde{f}_{\vec{e}_l}^t)^{(q_{\vec{e}_l})} \right] \right]_{i=1}^{k_{\vec{e}_l}} \in \mathbb{R}^{P_{\vec{e}_l} k_{\vec{e}_l} \times q_{\vec{e}_l}} \\ \left[ 0_{P_{\vec{e}_l}} \dots 0_{P_{\vec{e}_l}} \right]_{j=1}^{q_{\vec{e}_l} - k_{\vec{e}_l}} \end{bmatrix} \in \mathbb{R}^{P_{\vec{e}_l} q_{\vec{e}_l} \times q_{\vec{e}_l}} \quad (64)$$

and the matrix  $\tilde{\mathbf{Q}}_{\vec{e}_l} \in \mathbb{R}^{D_{\vec{e}_l} q_{\vec{e}_l} \times P_{\vec{e}_l} q_{\vec{e}_l}}$  is a dense Gaussian matrix with i.i.d. elements. Then

$$\tilde{\mathbf{Q}}_{\vec{e}_l} \tilde{F}_{\vec{e}_l}^t(\dots) = \begin{bmatrix} \sum_{j=1}^{k_{\vec{e}_l}} \mathbf{Q}_{\vec{e}_l}^{(j)} (\tilde{f}_{\vec{e}_l}^t)^{\lfloor j-1 \rfloor_{q_{\vec{e}_l}} + 1}(\dots) & \dots & \sum_{j=1}^{k_{\vec{e}_l}} (\mathbf{Q}_{\vec{e}_l}^{(j)} (\tilde{f}_{\vec{e}_l}^t)^{\lfloor j+q_{\vec{e}_l} - 2 \rfloor_{q_{\vec{e}_l}} + 1}(\dots)) \\ \vdots & & \vdots \\ \vdots & & \vdots \end{bmatrix} \in \mathbb{R}^{D_{\vec{e}_l} q_{\vec{e}_l} \times q_{\vec{e}_l}}$$

where each  $\dots$  is an identical copy of the first  $D_{\vec{e}_l} \times q_{\vec{e}_l}$  block, for a total of  $k_{\vec{e}_l}$  blocks. This means the  $D_{\vec{e}_l} q_{\vec{e}_l}$  output of the product  $\tilde{\mathbf{A}}_{\vec{e}_l} f_{\vec{e}_l}^t(\dots)$  may be rewritten as a  $D_{\vec{e}_l} \times q_{\vec{e}_l}$  matrix (copied  $k_{\vec{e}_l}$  times) resulting from the product of a dense Gaussian matrix with i.i.d. elements and a matrix valued function  $\tilde{F}_{\vec{e}_l}^t$  which verifies the same regularity conditions as  $f_{\vec{e}_l}^t$ . Note that, owing to the separability assumption, we may use any permutation of the  $(\tilde{f}_{\vec{e}_l}^t)^{(i)}$ ,  $1 \leq i \leq q_{\vec{e}_l}$  and will thus drop the permutations to write

$$\tilde{F}_{\vec{e}_l}^t(\dots) = \begin{bmatrix} \left[ (\tilde{f}_{\vec{e}_l}^t)^{(1)} \dots (\tilde{f}_{\vec{e}_l}^t)^{(q_{\vec{e}_l})} \right]_{i=1}^{k_{\vec{e}_l}} \in \mathbb{R}^{P_{\vec{e}_l} k_{\vec{e}_l} \times q_{\vec{e}_l}} \\ \left[ 0_{P_{\vec{e}_l}} \dots 0_{P_{\vec{e}_l}} \right]_{j=1}^{q_{\vec{e}_l} - k_{\vec{e}_l}} \end{bmatrix} \in \mathbb{R}^{P_{\vec{e}_l} q_{\vec{e}_l} \times q_{\vec{e}_l}} \quad (65)$$

Similarly, for products of the form  $(\tilde{\mathbf{A}}_{\vec{e}_l})^\top \tilde{f}_{\vec{e}_l}^t(\dots) \in \mathbb{R}^{P_{\vec{e}_l} q_{\vec{e}_l}}$ , we may write:

$$\begin{bmatrix} \mathbf{Q}_{\vec{e}_l}^{(1)} & \mathbf{Q}_{\vec{e}_l}^{(2)} & \dots & \mathbf{Q}_{\vec{e}_l}^{(k_{\vec{e}_l})} \\ & \mathbf{Q}_{\vec{e}_l}^{(1)} & \mathbf{Q}_{\vec{e}_l}^{(2)} & \dots & \mathbf{Q}_{\vec{e}_l}^{(k_{\vec{e}_l})} \\ & & \mathbf{Q}_{\vec{e}_l}^{(1)} & \mathbf{Q}_{\vec{e}_l}^{(2)} & \dots & \mathbf{Q}_{\vec{e}_l}^{(k_{\vec{e}_l})} \\ \vdots & \vdots & \ddots & & & \vdots \\ \mathbf{Q}_{\vec{e}_l}^{(2)} & \mathbf{Q}_{\vec{e}_l}^{(3)} & \dots & \mathbf{Q}_{\vec{e}_l}^{(k_{\vec{e}_l})} & & \mathbf{Q}_{\vec{e}_l}^{(1)} \end{bmatrix}^\top \begin{bmatrix} (\tilde{f}_{\vec{e}_l}^t)^{(1)}(\dots) \\ \vdots \\ (\tilde{f}_{\vec{e}_l}^t)^{(q_{\vec{e}_l})}(\dots) \end{bmatrix} \quad (66)$$

$$= \left[ \left( \mathcal{P}_{P_{\vec{e}_l}, q_{\vec{e}_l}} \right)^{i-1} \left[ (\mathbf{Q}_{\vec{e}_l}^{(1)})^\top (0 \dots 0) (\mathbf{Q}_{\vec{e}_l}^{(k_{\vec{e}_l})})^\top \dots (\mathbf{Q}_{\vec{e}_l}^{(2)})^\top \right] \right]_{i=1}^{q_{\vec{e}_l}} \tilde{f}_{\vec{e}_l}^t(\dots) \quad (67)$$

Then, using once again the separability assumption, we may define:

$$\tilde{F}_{\vec{e}_l}^t(\dots) = \begin{bmatrix} \left[ (\tilde{f}_{\vec{e}_l}^t)^{(1)} \dots (\tilde{f}_{\vec{e}_l}^t)^{(q_{\vec{e}_l})} \right]_{i=1}^{k_{\vec{e}_l}} \in \mathbb{R}^{D_{\vec{e}_l} k_{\vec{e}_l} \times q_{\vec{e}_l}} \\ \left[ 0_{D_{\vec{e}_l}} \dots 0_{D_{\vec{e}_l}} \right] \end{bmatrix} \in \mathbb{R}^{D_{\vec{e}_l} q_{\vec{e}_l} \times q_{\vec{e}_l}} \quad (68)$$

such that the term  $\tilde{\mathbf{Q}}_{\vec{e}_l}^\top \tilde{F}_{\vec{e}_l}^t(\dots)$  also contains  $k_{\vec{e}_l}$  copies of a  $P_{\vec{e}_l} \times q_{\vec{e}_l}$  block containing the  $q_{\vec{e}_l}$  blocks of size  $P_{\vec{e}_l}$  of the original  $P_{\vec{e}_l} q_{\vec{e}_l}$  vector  $\tilde{\mathbf{A}}_{\vec{e}_l}^\top \tilde{f}_{\vec{e}_l}^t(\dots)$ . The iterates of the sequences defined by Eq.(59)

may then be rewritten as a subset of the lines of the following matrix valued iteration, i.e.:

$$\begin{aligned}
\tilde{\mathbf{X}}_{e_1}^{t+1} &= \tilde{\mathbf{Q}}_{\rightarrow e_1} \tilde{\mathbf{M}}_{e_1}^t - b_{e_1}^t \tilde{\mathbf{M}}_{e_1}^{t-1}, \\
\tilde{\mathbf{M}}_{e_1}^t &= \tilde{F}_{\rightarrow e_1}^t(\tilde{\mathbf{X}}_{e_1}^t), \\
\tilde{\mathbf{X}}_{e_1}^{t+1} &= \tilde{\mathbf{Q}}_{\rightarrow e_1}^\top \tilde{\mathbf{M}}_{e_1}^t - b_{e_1}^t \tilde{\mathbf{M}}_{e_1}^{t-1}, \\
\tilde{\mathbf{M}}_{e_1}^t &= \tilde{F}_{e_1}^t \left( \tilde{\mathbf{Q}}_{\rightarrow e_1} \mathbf{W}_{\rightarrow e_1}, \tilde{\mathbf{X}}_{e_1}^t, \tilde{\mathbf{X}}_{e_2}^t \right), \\
\\
\tilde{\mathbf{X}}_{e_2}^{t+1} &= \tilde{\mathbf{Q}}_{\rightarrow e_2} \tilde{\mathbf{M}}_{e_2}^t - b_{e_2}^t \tilde{\mathbf{M}}_{e_2}^{t-1}, \\
\tilde{\mathbf{M}}_{e_2}^t &= \tilde{F}_{\rightarrow e_2}^t \left( \tilde{\mathbf{X}}_{e_1}^t, \tilde{\mathbf{X}}_{e_2}^t \right), \\
\tilde{\mathbf{X}}_{e_2}^{t+1} &= \tilde{\mathbf{Q}}_{\rightarrow e_2}^\top \tilde{\mathbf{M}}_{e_2}^t - b_{e_2}^t \tilde{\mathbf{M}}_{e_2}^{t-1}, \\
\tilde{\mathbf{M}}_{e_2}^t &= \tilde{F}_{e_2}^t \left( \tilde{\mathbf{Q}}_{\rightarrow e_2} \mathbf{W}_{\rightarrow e_2}, \tilde{\mathbf{X}}_{e_2}^t, \tilde{\mathbf{X}}_{e_3}^t \right), \\
\\
&\vdots \\
\\
\tilde{\mathbf{X}}_{e_L}^{t+1} &= \tilde{\mathbf{Q}}_{\rightarrow e_L} \tilde{\mathbf{M}}_{e_L}^t - b_{e_L}^t \tilde{\mathbf{M}}_{e_L}^{t-1}, \\
\tilde{\mathbf{M}}_{e_L}^t &= \tilde{F}_{\rightarrow e_L}^t \left( \tilde{\mathbf{X}}_{\rightarrow e_{L-1}}^t, \tilde{\mathbf{X}}_{e_L}^t \right), \\
\tilde{\mathbf{X}}_{e_L}^{t+1} &= \tilde{\mathbf{Q}}_{\rightarrow e_L}^\top \tilde{\mathbf{M}}_{e_L}^t - b_{e_L}^t \tilde{\mathbf{M}}_{e_L}^{t-1}, \\
\tilde{\mathbf{M}}_{e_L}^t &= \tilde{F}_{e_L}^t \left( \tilde{\mathbf{Q}}_{\rightarrow e_L} \mathbf{W}_{\rightarrow e_L}, \tilde{\mathbf{X}}_{e_L}^t \right)
\end{aligned} \tag{69}$$

where each  $\mathbf{W}_{\rightarrow e_l}$  contains  $k_{\rightarrow e_l}$  copies of the initial  $\mathbf{w}_{\rightarrow e_l}$  reorganised into matrices as described above. The dimensions of the variables are Note that at this point we have almost reached an iteration verifying the structure of that appearing in Theorem A.2, except the Onsager term isn't, a priori, the correct one. Consider the following iteration, where we replaced the original, scalar Onsager terms with the correct, matrix-valued ones:

$$\begin{aligned}
\tilde{\mathbf{X}}_{e_1}^{t+1} &= \tilde{\mathbf{Q}}_{\rightarrow e_1} \tilde{\mathbf{M}}_{e_1}^t - \tilde{\mathbf{M}}_{e_1}^{t-1} \left( \tilde{\mathbf{b}}_{e_1}^t \right)^\top, \\
\tilde{\mathbf{M}}_{e_1}^t &= \tilde{F}_{\rightarrow e_1}^t(\tilde{\mathbf{X}}_{e_1}^t), \\
\tilde{\mathbf{X}}_{e_1}^{t+1} &= \tilde{\mathbf{Q}}_{\rightarrow e_1}^\top \tilde{\mathbf{M}}_{e_1}^t - \tilde{\mathbf{M}}_{e_1}^{t-1} \left( \tilde{\mathbf{b}}_{e_1}^t \right)^\top, \\
\tilde{\mathbf{M}}_{e_1}^t &= \tilde{F}_{e_1}^t \left( \tilde{\mathbf{Q}}_{\rightarrow e_1} \mathbf{W}_{\rightarrow e_1}, \tilde{\mathbf{X}}_{e_1}^t, \tilde{\mathbf{X}}_{e_2}^t \right), \\
\\
\tilde{\mathbf{X}}_{e_2}^{t+1} &= \tilde{\mathbf{Q}}_{\rightarrow e_2} \tilde{\mathbf{M}}_{e_2}^t - \tilde{\mathbf{M}}_{e_2}^{t-1} \left( \tilde{\mathbf{b}}_{e_2}^t \right)^\top, \\
\tilde{\mathbf{M}}_{e_2}^t &= \tilde{F}_{\rightarrow e_2}^t \left( \tilde{\mathbf{X}}_{e_1}^t, \tilde{\mathbf{X}}_{e_2}^t \right), \\
\tilde{\mathbf{X}}_{e_2}^{t+1} &= \tilde{\mathbf{Q}}_{\rightarrow e_2}^\top \tilde{\mathbf{M}}_{e_2}^t - \tilde{\mathbf{M}}_{e_2}^{t-1} \left( \tilde{\mathbf{b}}_{e_2}^t \right)^\top, \\
\tilde{\mathbf{M}}_{e_2}^t &= \tilde{F}_{e_2}^t \left( \tilde{\mathbf{Q}}_{\rightarrow e_2} \mathbf{W}_{\rightarrow e_2}, \tilde{\mathbf{X}}_{e_2}^t, \tilde{\mathbf{X}}_{e_3}^t \right)
\end{aligned} \tag{70}$$

⋮

$$\begin{aligned}
\tilde{\mathbf{X}}_{e_L}^{t+1} &= \tilde{\mathbf{Q}}_{\vec{e}_L} \tilde{\mathbf{M}}_{e_L}^t - \tilde{\mathbf{M}}_{e_L}^{t-1} \left( \tilde{\mathbf{b}}_{e_L}^t \right)^\top, \\
\tilde{\mathbf{M}}_{e_L}^t &= \tilde{F}_{\vec{e}_L}^t \left( \tilde{\mathbf{X}}_{\vec{e}_{L-1}}^t, \tilde{\mathbf{X}}_{e_L}^t \right), \\
\tilde{\mathbf{X}}_{e_L}^{t+1} &= \tilde{\mathbf{Q}}_{\vec{e}_L}^\top \tilde{\mathbf{M}}_{e_L}^t - \tilde{\mathbf{M}}_{e_L}^{t-1} \left( \tilde{\mathbf{b}}_{e_L}^t \right)^\top, \\
\tilde{\mathbf{M}}_{e_L}^t &= \tilde{F}_{e_L}^t \left( \tilde{\mathbf{Q}}_{\vec{e}_L} \mathbf{W}_{\vec{e}_L}, \tilde{\mathbf{X}}_{e_L}^t \right)
\end{aligned} \tag{71}$$

where, for any  $\vec{e} \in \vec{E}$  and any  $t \in \mathbb{N}$  for the right oriented edges

$$\mathbf{b}_{\vec{e}_l}^t = \frac{1}{N} \sum_{i=1}^{n_{l-1}} \frac{\partial \tilde{F}_{\vec{e}_l, i}^t}{\partial \mathbf{X}_{\vec{e}_l, i}^t} \left( \left( \mathbf{X}_{\vec{e}_l}^t \right)_{\vec{e}_l'; \vec{e}_l' \rightarrow \vec{e}_l} \right) \in \mathbb{R}^{q_{\vec{e}_l} \times q_{\vec{e}_l}}.$$

and left oriented edges

$$\mathbf{b}_{\vec{e}_l}^t = \frac{1}{N} \sum_{i=1}^{n_l} \frac{\partial \tilde{F}_{\vec{e}_l, i}^t}{\partial \mathbf{X}_{\vec{e}_l, i}^t} \left( \tilde{\mathbf{Q}}_{\vec{e}_l} \mathbf{W}_{\vec{e}_l}, \left( \mathbf{X}_{\vec{e}_l}^t \right)_{\vec{e}_l'; \vec{e}_l' \rightarrow \vec{e}_l} \right) \in \mathbb{R}^{q_{\vec{e}_l} \times q_{\vec{e}_l}}.$$

Using the separability assumption, we can simplify this expression. To take a concrete example, consider  $\tilde{F}_{\vec{e}_2}^t \left( \tilde{\mathbf{X}}_{\vec{e}_1}^t, \tilde{\mathbf{X}}_{\vec{e}_2}^t \right)$ . Let's start with the dimensions. Recall

$$\tilde{f}_{\vec{e}_2}^t \left( \tilde{\mathbf{x}}_{\vec{e}_1}^t, \tilde{\mathbf{x}}_{\vec{e}_2}^t \right) \in \mathbb{R}^{P_{\vec{e}_2} q_{\vec{e}_2}} = \mathbf{V}_{\vec{e}_2}^\top f_{\vec{e}_2}^t \left( \mathbf{U}_{\vec{e}_1} \tilde{\mathbf{x}}_{\vec{e}_1}^t, \mathbf{V}_{\vec{e}_2} \tilde{\mathbf{x}}_{\vec{e}_2}^t \right) \tag{72}$$

$$\text{where } \tilde{\mathbf{x}}_{\vec{e}_1}^t \in \mathbb{R}^{D_{\vec{e}_1} q_{\vec{e}_1}} = \mathbb{R}^{P_{\vec{e}_2} q_{\vec{e}_2}} \text{ and } \tilde{\mathbf{x}}_{\vec{e}_2}^t \in \mathbb{R}^{P_{\vec{e}_2} q_{\vec{e}_2}} \tag{73}$$

using the separability assumption, we may write

$$\forall 1 \leq i \leq P_{\vec{e}_2} q_{\vec{e}_2} \tag{74}$$

$$\left( f_{\vec{e}_2}^t \left( \mathbf{U}_{\vec{e}_1} \tilde{\mathbf{x}}_{\vec{e}_1}^t, \mathbf{V}_{\vec{e}_2} \tilde{\mathbf{x}}_{\vec{e}_2}^t \right) \right)_i = \sigma_{\vec{e}_2}^t \left( \left( \mathbf{U}_{\vec{e}_1} \tilde{\mathbf{x}}_{\vec{e}_1}^t \right)_i, \left( \mathbf{V}_{\vec{e}_2} \tilde{\mathbf{x}}_{\vec{e}_2}^t \right)_i \right) \tag{75}$$

And

$$\tilde{F}_{\vec{e}_2}^t \left( \tilde{\mathbf{X}}_{\vec{e}_1}^t, \tilde{\mathbf{X}}_{\vec{e}_2}^t \right) \in \mathbb{R}^{P_{\vec{e}_2} q_{\vec{e}_2} \times q_{\vec{e}_2}} \tag{76}$$

$$\text{where } \tilde{\mathbf{X}}_{\vec{e}_1}^t \in \mathbb{R}^{P_{\vec{e}_2} q_{\vec{e}_2} \times q_{\vec{e}_2}} \text{ and } \tilde{\mathbf{X}}_{\vec{e}_2}^t \in \mathbb{R}^{P_{\vec{e}_2} q_{\vec{e}_2} \times q_{\vec{e}_2}} \tag{77}$$

$$\tilde{F}_{\vec{e}_2}^t \left( \tilde{\mathbf{X}}_{\vec{e}_1}^t, \tilde{\mathbf{X}}_{\vec{e}_2}^t \right) = \left[ \left[ \left( \tilde{f}_{\vec{e}_1}^t \right)^{(1)} \left( \tilde{\mathbf{x}}_{\vec{e}_1}^{t,(1)}, \tilde{\mathbf{x}}_{\vec{e}_2}^{t,(1)} \right) \dots \left( \tilde{f}_{\vec{e}_1}^t \right)^{(q_{\vec{e}_1})} \left( \tilde{\mathbf{x}}_{\vec{e}_1}^{t,(q_{\vec{e}_1})}, \tilde{\mathbf{x}}_{\vec{e}_2}^{t,(q_{\vec{e}_1})} \right) \right]_{i=1}^{k_{\vec{e}_2}} \right] \tag{78}$$

$$= \left[ \left( \tilde{g}_{\vec{e}_1}^t \right)^{(1)} \left( \tilde{\mathbf{x}}_{\vec{e}_1}^{t,(1)}, \tilde{\mathbf{x}}_{\vec{e}_2}^{t,(1)} \right) \dots \left( \tilde{g}_{\vec{e}_1}^t \right)^{(q_{\vec{e}_1})} \left( \tilde{\mathbf{x}}_{\vec{e}_1}^{t,(q_{\vec{e}_1})}, \tilde{\mathbf{x}}_{\vec{e}_2}^{t,(q_{\vec{e}_1})} \right) \right]_{i=1}^{q_{\vec{e}_2}} \tag{79}$$

where each  $\tilde{\mathbf{x}}_{\vec{e}_2}^{t,(i)} \in \mathbb{R}^{P_{\vec{e}_2} q_{\vec{e}_2}}$ . Recall that, for any  $1 \leq i \leq Pk$ ,  $\tilde{F}_{\vec{e}_2, i}^t : \mathbb{R}^{q_{\vec{e}_2}} \rightarrow \mathbb{R}^{q_{\vec{e}_2}}$ . Then, for any

$1 \leq k, l \leq q_{\vec{e}_2}$

$$\left(\tilde{\mathbf{b}}_{\vec{e}_2}^t\right)_{k,l} = \frac{1}{N} \sum_{i=1}^{P_{\vec{e}_2} q_{\vec{e}_2}} \frac{\partial \tilde{F}_{\vec{e}_2,i}^t}{\partial \mathbf{X}_{\vec{e}_2,i}^t} \left(\tilde{\mathbf{X}}_{\vec{e}_1}^t, \tilde{\mathbf{X}}_{\vec{e}_2}^t\right) \quad (80)$$

$$= \frac{1}{N} \sum_{i=1}^{P_{\vec{e}_2} q_{\vec{e}_2}} \frac{\partial (\tilde{g}_{\vec{e}_2,i}^t)^{(k)}}{\partial \tilde{\mathbf{x}}_{\vec{e}_2,i}^{t,(l)}} \left(\tilde{\mathbf{x}}_{\vec{e}_1}^{t,(k)}, \tilde{\mathbf{x}}_{\vec{e}_2}^{t,(k)}\right) \quad (81)$$

$$= \frac{1}{N} \sum_{i=1}^{P_{\vec{e}_2} q_{\vec{e}_2}} \frac{\partial}{\partial \tilde{\mathbf{x}}_{\vec{e}_2}^{t,(l)}} \mathbf{V}_{\vec{e}_2}^\top (g_{\vec{e}_2}^t)^{(k)} \left(\mathbf{U}_{\vec{e}_1} \tilde{\mathbf{x}}_{\vec{e}_1}^{t,(l)}, \mathbf{V}_{\vec{e}_2} \tilde{\mathbf{x}}_{\vec{e}_2}^{t,(l)}\right) \quad (82)$$

$$= \frac{1}{N} \text{Tr} \left( \mathbf{V}_{\vec{e}_2}^\top \mathcal{J}_{(g_{\vec{e}_2}^t)^{(k)}} \left(\mathbf{U}_{\vec{e}_1} \tilde{\mathbf{x}}_{\vec{e}_1}^{t,(l)}, \mathbf{V}_{\vec{e}_2} \tilde{\mathbf{x}}_{\vec{e}_2}^{t,(l)}\right) \mathbf{V}_{\vec{e}_2} \right) \delta_{k,l} \quad (83)$$

$$= \frac{1}{N} \text{Tr} \left( \mathcal{J}_{(g_{\vec{e}_2}^t)} \left(\mathbf{U}_{\vec{e}_1} \tilde{\mathbf{x}}_{\vec{e}_1}^t, \mathbf{V}_{\vec{e}_2} \tilde{\mathbf{x}}_{\vec{e}_2}^t\right) \right) \delta_{k,l} \quad (84)$$

$$= \frac{1}{N} \sum_{i=1}^{P_{\vec{e}_2} q_{\vec{e}_2}} (\sigma^t)'_{\vec{e}_2} \left( \left(\mathbf{U}_{\vec{e}_1} \tilde{\mathbf{x}}_{\vec{e}_1}^t\right)_i, \left(\mathbf{V}_{\vec{e}_2} \tilde{\mathbf{x}}_{\vec{e}_2}^t\right)_i \right) \delta_{k,l} \quad (85)$$

where we wrote  $\mathcal{J}_{(g_{\vec{e}_2}^t)^{(k)}}$  the  $N \times N$  Jacobian matrix of the function  $(g_{\vec{e}_2}^t)^{(k)} : \mathbb{R}^N \rightarrow \mathbb{R}^N$ . Using [Berthier et al., 2020] corollary 2, the Onsager term can be replaced by any estimator based on the asymptotically Gaussian iterates converging, in the high-dimensional limit, to the correct expectation. The adaptation to the graph framework of [Gerbelot and Berthier, 2021] is immediate (see the proof in [Berthier et al., 2020] and corresponding comment in [Gerbelot and Berthier, 2021]). Using the permutation invariance of the Gaussian distribution, we can therefore replace each element of the matrix the Onsager term with

$$\frac{1}{P_{\vec{e}_2} q_{\vec{e}_2}} \sum_{i=1}^{P_{\vec{e}_2} q_{\vec{e}_2}} (\sigma^t)'_{\vec{e}_2} \left( \left(\tilde{\mathbf{x}}_{\vec{e}_1}^t\right)_i, \left(\tilde{\mathbf{x}}_{\vec{e}_2}^t\right)_i \right) \delta_{k,l} \quad (86)$$

which amounts to

$$\tilde{\mathbf{b}}_{\vec{e}_2}^t = b_{\vec{e}_2}^t \mathbf{I}_{q_{\vec{e}_2} \times q_{\vec{e}_2}} \quad (87)$$

We therefore obtain an exact reformulation of the initial MLAMP iteration with convolutional matrices in terms of a subset (first line of size  $P_{\vec{e}_l} \times q_{\vec{e}_l}$  for right oriented edges and  $D_{\vec{e}_l} \times q_{\vec{e}_l}$  for left-oriented variables) of the variables of a matrix-valued iteration with dense Gaussian matrices verifying the SE equations. Isolating the aforementioned first lines, recalling that the SE equations prescribes i.i.d. lines in the asymptotically Gaussian fields, we recover that, for any  $1 \leq l \leq L$ , the variable  $\mathbf{x}_{\vec{e}_l} \in \mathbb{R}^{P_{\vec{e}_l} q_{\vec{e}_l}}$  is composed of  $q_{\vec{e}_l}$  copies of block of size  $P_{\vec{e}_l}$  with i.i.d. Gaussian elements distributed according to the SE equations (A.3). The distribution of the variables associated to left-oriented edges is obtained similarly. Note that, from a finite size point of view, the effect of  $D_{\vec{e}_l}, P_{\vec{e}_l}$  is different from that of  $q_{\vec{e}_l}$ : the former results in subGaussian concentration i.e. exponential in the dimension, while the latter only represents copies (and not i.i.d. samples), and thus only has an averaging effect. This is observed in simulations.  $\square$

#### A.4 Bayes-optimal MLAMP with random convolutional matrices

In this section, we specialize the equations obtained in the previous section to the Bayes-optimal MLAMP iteration of the main body of the paper. Several functions are reminded for convenience. Consider the MLAMP iteration outlined in section 3.3. The scalar updates described in Eq.(4) can be rewritten as

vector-valued updates as follows, for any  $t \in \mathbb{N}$ , and any  $0 \leq l \leq L$ :

$$\boldsymbol{\omega}^{(l)}(t) = \mathbf{W}^{(l)} \hat{\mathbf{h}}^{(l)}(t) - V^{(l)}(t) \mathbf{g}^{(l)}(t-1) \quad (88)$$

$$\mathbf{B}^{(l)}(t) = \left( \mathbf{W}^{(l)} \right)^\top \mathbf{g}^{(l)}(t) - \hat{V}^{(l)}(t) \hat{\mathbf{h}}(t). \quad (89)$$

To define the update functions and terms  $V^{(l)}$ ,  $\hat{V}^{(l)}$ , the following partition functions were introduced.

- for  $l = 1$

$$\mathcal{Z}^{(1)}(y, V^{(1)}, \omega^{(1)}) = \frac{1}{\sqrt{2\pi V^{(1)}}} \int dz P_{out}^{(1)}(y|z) e^{-\frac{(z-\omega^{(1)})^2}{2V^{(1)}}} \quad (90)$$

- for any  $2 \leq l \leq L-1$ :

$$\begin{aligned} \mathcal{Z}^{(l)}(A^{(l-1)}, B^{(l-1)}, V^{(l)}, \omega^{(l)}) = \\ \frac{1}{\sqrt{2\pi V^{(l)}}} \int dh dz P_{out}^{(l)}(h|z) e^{-\frac{1}{2}A^{(l-1)}h^2 + B^{(l-1)}h} e^{-\frac{(z-\omega^{(l)})^2}{2V^{(l)}}} \end{aligned} \quad (91)$$

- for  $l = L$

$$\mathcal{Z}^{(L)}(A^{(L)}, B^{(L)}) = \int dh P_X(h) e^{-\frac{1}{2}A^{(L)}h^2 + B^{(L)}h} \quad (92)$$

We then define the layer-dependent, time-dependent, scalar update functions  $f^{(l),t}$ ,  $\tilde{f}^{(l),t}$

$$\forall (B, \omega) \in \mathbb{R}^2$$

$$f^{(1),t}(\omega) = \partial_\omega \log \mathcal{Z}^{(1)}(y, V^{(1)}(t), \omega) \quad (93)$$

$$f^{(l),t}(B, \omega) = \partial_\omega \log \mathcal{Z}^{(l)}(A^{(l-1)}(t), B, V^{(l)}(t), \omega) \quad 2 \leq l \leq L \quad (94)$$

$$\tilde{f}^{(l),t}(B, \omega) = \partial_B \log \mathcal{Z}^{(l+1)}(A^{(l)}(t-1), B, V^{(l+1)}(t-1), \omega) \quad 1 \leq l \leq L-1 \quad (95)$$

$$\tilde{f}^{(L),t}(B) = \partial_B \log \mathcal{Z}^{(L+1)}(A^{(L)}(t-1), B), \quad (96)$$

and their corresponding separable, vector valued counterparts  $\mathbf{f}^{(l)}$ ,  $\tilde{\mathbf{f}}^{(l)}$ , which leads to the following iteration

$$\boldsymbol{\omega}^{(l)}(t) = \mathbf{W}^{(l)} \tilde{\mathbf{f}}^{(l),t}(\mathbf{B}^{(l),t-1}, \boldsymbol{\omega}^{(l+1),t-1}) - V^{(l)}(t) \mathbf{f}^{(l),t-1}(\mathbf{B}^{(l-1),t-1}, \boldsymbol{\omega}^{(l),t-1}) \quad (97)$$

$$\mathbf{B}^{(l)}(t) = \left( \mathbf{W}^{(l)} \right)^\top \mathbf{f}^{(l),t}(\mathbf{B}^{(l-1),t}, \boldsymbol{\omega}^{(l),t}) - \hat{V}^{(l)}(t) \tilde{\mathbf{f}}^{(l),t}(\mathbf{B}^{(l),t-1}, \boldsymbol{\omega}^{(l+1),t-1}), \quad (98)$$

where the Onsager terms  $V^{(l),t}$  and  $\hat{V}^{(l),t}$  reduce to, using the separability of the update functions,

$$V^{(l),t} = \frac{1}{n_l} \sum_{i=1}^{n_{l-1}} \partial_B \tilde{f}^{(l),t}(B_i^{(l),t-1}, \omega_i^{(l+1),t-1}) \quad (99)$$

$$\hat{V}^{(l),t} = \frac{1}{n_l} \sum_{j=1}^{n_l} \partial_\omega f^{(l),t}(B_j^{(l-1),t}, \omega_j^{(l),t}) = -A^{(l),t} \quad (100)$$

We now show that the update functions defined above are Lipschitz continuous and increasing, thus ensuring that the integrals are well defined through positivity of the parameters  $V$ ,  $\hat{V}$ .

**Lemma A.4.** For any  $1 \leq l \leq L$ , and any  $t \in \mathbb{N}$ , the functions  $f^{(l),t}$ ,  $\tilde{f}^{(l),t}$  are Lipschitz continuous in  $B, \omega$ . Furthermore, the functions  $f^{(l),t}$ ,  $\tilde{f}^{(l),t}$  are respectively decreasing in  $\omega$  and increasing in  $B$ . As a consequence, the variance terms  $A^{(l),t}$  and  $V^{(l),t}$  are strictly positive.

*Proof.* Recall the partition function, omitting the layer index since all regularity assumptions are the same for all layers and time indices,

$$\mathcal{Z}(A, B, V, \omega) := \frac{1}{\sqrt{2\pi V}} \int P(h | z) \exp\left(Bh - \frac{1}{2}Ah^2 - \frac{(z - \omega)^2}{2V}\right) dh dz \quad (101)$$

recalling  $p(h|z) = \int p(\xi)\delta(h - f_\xi(z))d\xi$ , integrating in  $h$  yields

$$\mathcal{Z}(A, B, V, \omega) := \frac{1}{\sqrt{2\pi V}} \int P(\xi) \exp\left(Bf_\xi(z) - \frac{1}{2}Af_\xi(z)^2 - \frac{(z - \omega)^2}{2V}\right) d\xi dz \quad (102)$$

Starting with  $\tilde{f}$ , we can straightforwardly verify the conditions to apply the dominated convergence theorem and differentiate under the integral to obtain

$$\begin{aligned} \partial_B \tilde{f}(B, \omega) &= \partial_B^2 \log(\mathcal{Z}(A, B, V, \omega)) \\ &= \frac{1}{(\sqrt{2\pi V} \mathcal{Z}(A, B, V, \omega))^2} \left( \int P(\xi) f_\xi^2(z) \exp\left(Bf_\xi(z) - \frac{1}{2}Af_\xi(z)^2 - \frac{(z - \omega)^2}{2V}\right) d\xi dz \times \right. \\ &\quad \left. \int P(\xi) \exp\left(Bf_\xi(z) - \frac{1}{2}Af_\xi(z)^2 - \frac{(z - \omega)^2}{2V}\right) d\xi dz - \right. \\ &\quad \left. \left( \int P(\xi) f_\xi(z) \exp\left(Bf_\xi(z) - \frac{1}{2}Af_\xi(z)^2 - \frac{(z - \omega)^2}{2V}\right) d\xi dz \right)^2 \right) \geq 0 \quad (103) \end{aligned}$$

where the positivity comes from the Cauchy-Schwarz inequality and positivity of the term  $P(\xi) \exp\left(Bf_\xi(z) - \frac{1}{2}Af_\xi(z)^2 - \frac{(z - \omega)^2}{2V}\right)$ .

Turning to  $f$ , we complete the square in the variable  $h$  to obtain

$$\mathcal{Z}(A, B, V, \omega) := \frac{\exp\left(\frac{B^2}{2A}\right)}{\sqrt{2\pi V}} \int P(\xi) \exp\left(-\frac{A}{2}\left(f_\xi(z) - \frac{B}{A}\right)^2\right) \exp\left(-\frac{(z - \omega)^2}{2V}\right) d\xi dz \quad (104)$$

and differentiating under the integral yields

$$f(B, \omega) = \partial_\omega \log(\mathcal{Z}(A, B, V, \omega)) \quad (105)$$

$$= \frac{1}{V} \left( \frac{\int P(\xi) z \exp\left(-\frac{A}{2}\left(f_\xi(z) - \frac{B}{A}\right)^2\right) \exp\left(-\frac{(z - \omega)^2}{2V}\right) d\xi dz}{\int P(\xi) \exp\left(-\frac{A}{2}\left(f_\xi(z) - \frac{B}{A}\right)^2\right) \exp\left(-\frac{(z - \omega)^2}{2V}\right) d\xi dz} - \omega \right) \quad (106)$$

where the term  $\frac{\int P(\xi) z \exp\left(-\frac{A}{2}\left(f_\xi(z) - \frac{B}{A}\right)^2\right) \exp\left(-\frac{(z - \omega)^2}{2V}\right) d\xi dz}{\int P(\xi) \exp\left(-\frac{A}{2}\left(f_\xi(z) - \frac{B}{A}\right)^2\right) \exp\left(-\frac{(z - \omega)^2}{2V}\right) d\xi dz}$  is the conditional mean of the distribution

with density  $\frac{\int P(\xi) \exp\left(-\frac{A}{2}\left(f_\xi(z) - \frac{B}{A}\right)^2\right) \exp\left(-\frac{(z - \omega)^2}{2V}\right) d\xi}{\int P(\xi) \exp\left(-\frac{A}{2}\left(f_\xi(z) - \frac{B}{A}\right)^2\right) \exp\left(-\frac{(z - \omega)^2}{2V}\right) d\xi dz}$ . The Lipschitz property is straightforward to verify using the polynomial bound assumption on the activation functions and the inverse exponential factors.  $\square$

In the Bayes-optimal MLAMP, see [Manoel et al., 2017], the planted vectors  $\mathbf{w}_{\vec{e}_l}$  are chosen as independently distributed as the asymptotic SE representation of the output of the previous layer, and are therefore Lipschitz transforms of subGaussian random variables, and thus are also subgaussian. Using the permutation invariance of the Gaussian distribution, the quantities  $\mathbf{z}_{\vec{e}_l} = \hat{\mathbf{A}}_{\vec{e}_l}$  remain Gaussian. We can therefore apply the result of Lemma A.3 to this iteration and obtain that iterates of Eq.(4) verify the SE equations from Lemma A.3 with the corresponding update functions. Furthermore, in the Bayes optimal case, the Nishimori conditions, see e.g. [Krzakala et al., 2012], allow to only keep the parameters  $\nu_{\vec{e}_l}, \hat{\nu}_{\vec{e}_l}$  to describe the distribution of the iterates, recovering the equations of Theorem 4.2. Finally, the rescaling of the variances to go from the factors  $\delta_l$  to the  $\beta_l$  of the main can be done by rescaling each non-linearity  $f_{\vec{e}_l}^t$  by  $\sqrt{N/n_{l-1}}$  (and similarly for the  $f_{\vec{e}_l}^t$  with  $\sqrt{N/n_l}$ ) as done in [Javanmard and Montanari, 2013; Berthier et al., 2020].

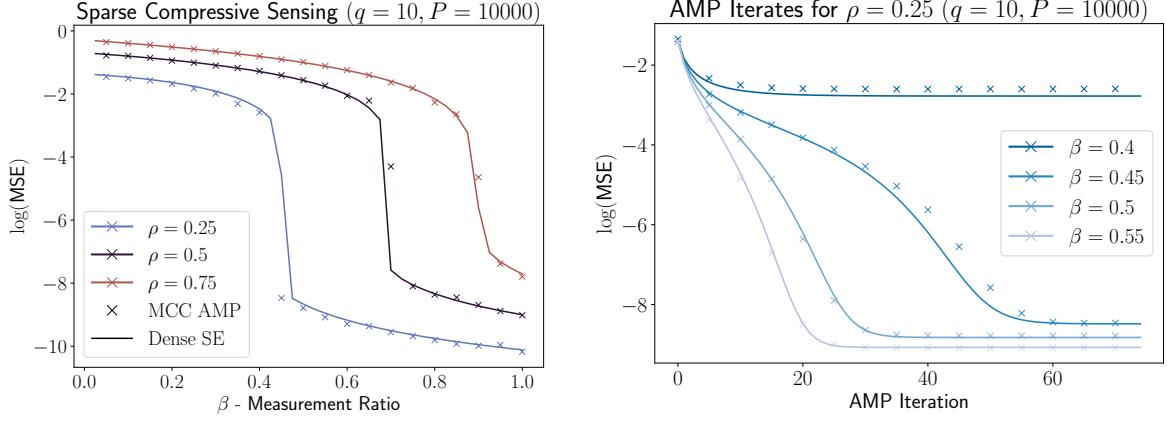


Figure 6: Replica of Figure 1 for  $q = 10$  and  $P = 10000$ . **(left)** Compressive sensing  $y_0 = Wx_0 + \zeta$  for noise  $\zeta_i \sim \mathcal{N}(0, 10^{-4})$  and signal prior  $x_0 \sim \rho\mathcal{N}(0, 1) + (1 - \rho)\delta(x)$ , where  $W \in \mathbb{R}^{Dq \times Pq}$  has varying aspect ratio  $\beta = D/P$ . Crosses correspond to AMP evaluations for  $W \sim \text{MCC}(D, P, q, k)$  according to Definition 3.2, averaged over 10 independent trials. Lines show the state evolution predictions when  $W_{ij} \sim \mathcal{N}(0, 1/Pq)$ . The system size is  $P = 10000$ ,  $q = 10$ ,  $k = 3$ , where  $\beta$  and  $D = \beta P$  vary. **(right)** AMP iterates at  $\rho = 0.25$  and  $\beta$  near the recovery transition.

## B Fast MCC-vector Products

Here is a simple sketch of an algorithm for multiplying  $M \sim \text{MCC}(D, P, q, k)$  with a vector  $v \in \mathbb{R}^{Pq}$  that runs in time  $O(DPq \log q)$ . If  $k \gg \log q$ , this improves on the runtime required by a simple sparse matrix-vector product. We use Matlab index notation for matrix and vector coordinates, for example  $M[i : j, k] = [M_{rk} : r = i \dots j]$ , and we write shorthand  $M_{ij}$  for  $M[i, j]$ .

---

**Algorithm 1:**  $O(DPq \log q)$  time algorithm for MCC-vector products

**Data:** matrix  $M \sim \text{MCC}(D, P, q, k)$ , vector  $v \in \mathbb{R}^{Pq}$

Initialize  $s \in \mathbb{R}^{Dq}$  the zero vector;

**for**  $i = 1 \dots D$  **do**

**for**  $j = 1 \dots P$  **do**

$C_{ij} \leftarrow M[qi : q(i+1), qj : q(j+1)];$

$\omega_{ij} = C_{ij}[0, 0 : k];$

$\hat{\omega}_{ij} = \text{FFT}(\omega_{ij});$

$\hat{v}_j = \text{FFT}(v[qj, q(j+1)]);$

$\hat{s}_i = \hat{\omega}_{ij} * \hat{v}_j;$

$s[qi : q(i+1)] = \text{IFFT}(\hat{s}_i);$

## C Additional Experiments

### C.1 Sparse Compressive Sensing

We observe empirically that in the sparse compressive sensing task of Figure 1, the relative sizes of  $(D, P)$  and  $q$  have little impact on the performance of the corresponding AMP iteration. In Figure 6, we show a replica of this figure with  $q = 10$  and  $P = 10000$ . Despite a significant difference between the relative sizes of these parameters, the AMP iterations behave largely the same.

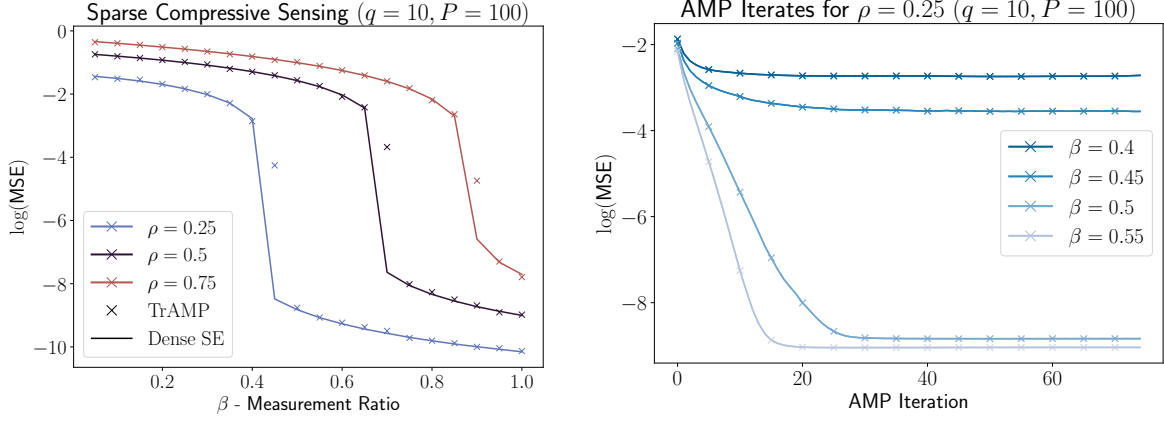


Figure 7: Replica of Figure 1 using Tree-AMP [Baker et al., 2020], a compositional VAMP type algorithm, for  $q = 10$  and  $P = 100$ . **(left)** Compressive sensing  $y_0 = Wx_0 + \zeta$  for noise  $\zeta_i \sim \mathcal{N}(0, 10^{-4})$  and signal prior  $x_0 \sim \rho\mathcal{N}(0, 1) + (1 - \rho)\delta(x)$ , where  $W \in \mathbb{R}^{Dq \times Pq}$  has varying aspect ratio  $\beta = D/P$ . Crosses correspond to AMP evaluations for  $W \sim \text{MCC}(D, P, q, k)$  according to Definition 3.2, averaged over 30 independent trials. Lines show the state evolution predictions when  $W_{ij} \sim \mathcal{N}(0, 1/Pq)$ . The system size is  $P = 100, q = 10, k = 3$ , where  $\beta$  and  $D = \beta P$  vary. **(right)** AMP iterates at  $\rho = 0.25$  and  $\beta$  near the recovery transition.

## C.2 Empirical Results for Vector-AMP Algorithms

We observe that a similar equivalence property as Theorem 4.2 holds for algorithms based on the VAMP framework [Schniter et al., 2016; Fletcher et al., 2018; Baker et al., 2020]. Previously, state evolution has been proven for such algorithms when their sensing matrices are drawn from a right-orthogonally-invariant ensemble. While the random MCC ensemble does not satisfy this property, we show in Figure 7 a comparison between empirical VAMP performance and the corresponding SE predictions for dense matrices, which are almost identical.

## D Structured Convolutions and Non-separable Denoising

Our proof uses a relatively simple version of spatial coupling, leaving avenues for potential generalizations. Spatially coupled sensing matrices typically consist of a block structured matrix whose blocks are i.i.d. Gaussian with different variances, as in (for instance) [Krzakala et al., 2012; Barbier et al., 2015]. As a model, consider  $\tilde{M}_{\text{sp}}$  of the following form, with variances  $\kappa \in \mathbb{R}_+^{q \times q}$ ,

$$\tilde{M}_{\text{sp}} = \begin{bmatrix} \kappa_{11}A_{11} & \kappa_{12}A_{12} & \dots & \kappa_{1q}A_{1q} \\ \kappa_{21}A_{21} & \ddots & & \vdots \\ \vdots & & & \\ \kappa_{1q}A_{1q} & \dots & & \kappa_{qq}A_{qq} \end{bmatrix}.$$

As a result of Lemma 4.3, a given MCC matrix  $M$  is equivalent to  $\tilde{M}$  corresponding to the case where  $\kappa$  is a convolutional matrix according to Definition 3.1, with filter  $\omega = [1 \ 1 \ \dots \ 1] \in \mathbb{R}^k$ . One avenue to extend our results is to consider general  $\tilde{M}$  where  $\kappa$  is any circulant matrix. Inverting the permutation lemma, this corresponds to MCC matrices whose convolutional blocks have filters with independent non-isotropic coordinates, as in the following definition, which may be viewed as a simple model for structured convolutional filters.



**Definition D.1** (Independent Gaussian Random Convolutions). Let  $\vec{\kappa} = [\kappa_1, \dots, \kappa_k] \in \mathbb{R}_+^k$  and let  $\Sigma = \text{diag}(\vec{\kappa})$ . Let  $q \geq k > 0$  be integers. The Gaussian convolutional ensemble  $\mathcal{C}(q, k)$  contains random circulant matrices  $C \in \mathbb{R}^{q \times q}$  whose first rows are given by  $C_1 = \text{zero-pad}_{q,k}[\omega]$  where  $\omega \sim \mathcal{N}(0, \Sigma)$ .

This model is a natural extension of our current setting, which is also amenable to proof techniques designed for spatial coupling. However, because the nonzero coordinates of the sensing matrix are no longer i.i.d., the Bayes-optimal denoising functions corresponding to this problem are non-separable. So, an equivalence theorem analogous to Theorem 4.2 is not expected to hold – in other words, state evolution in this convolutional model is not expected to reduce to that of a signal model with dense i.i.d. couplings. More generally, multilayer AMP iterations with non-separable non-linearities may be written to compute marginals of posterior distributions involving such functions, and will verify SE equations. However there will be no direct correspondance with the iteration and SE equations of the fully separable case.